

„History of solar activity recorded in polar ice“
Dübendorf/Zürich, 14-15 November 2016

What can we learn from liquid metal experiments on dynamo action and magnetically triggered instabilities?

Frank Stefani

with thanks to

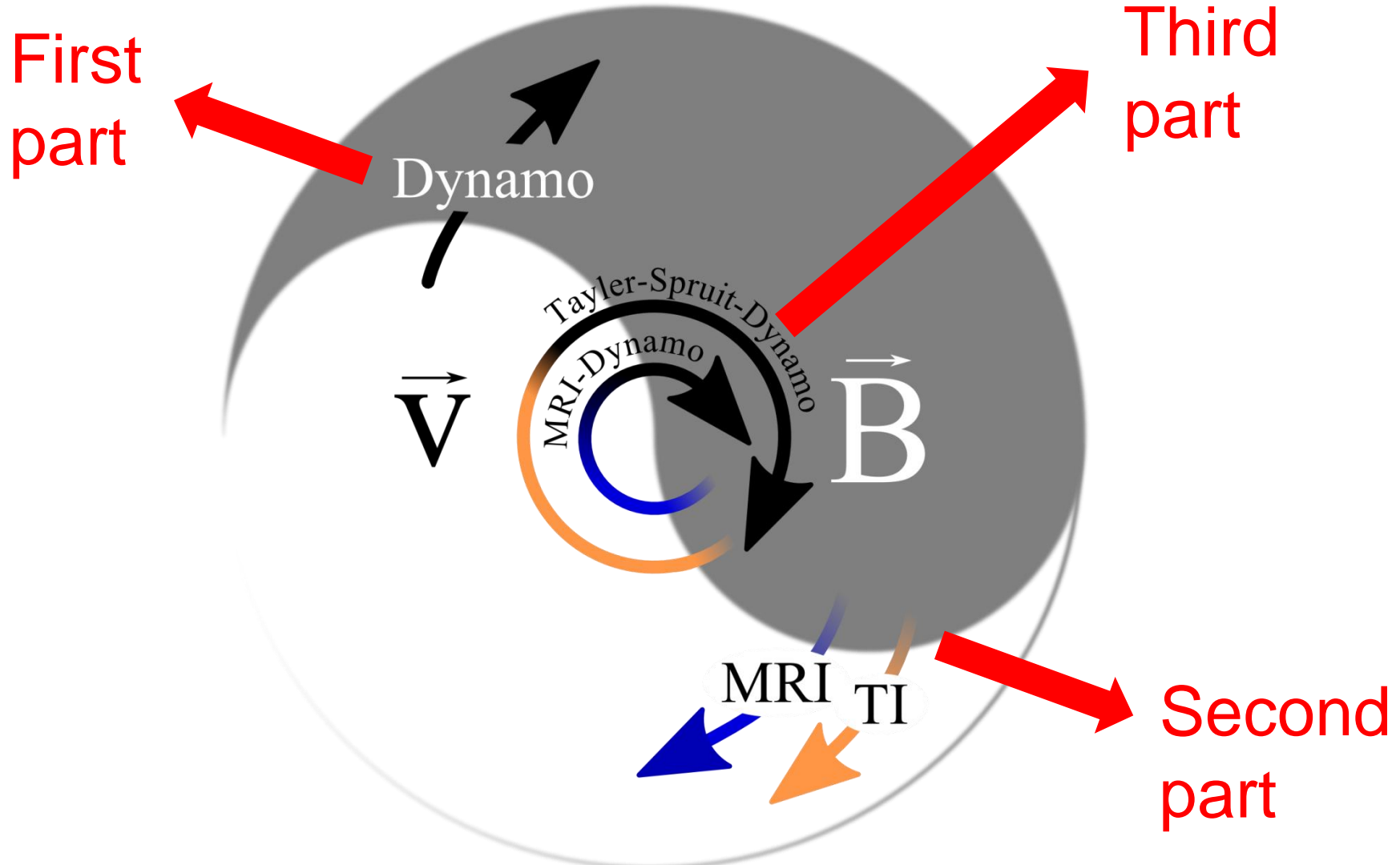
**G. Gerbeth, A. Giesecke, Th. Gundrum, G. Mamatsashvili ,
Ch. Steglich, M. Seilmayer, N. Weber, T. Weier (Dresden)**

G. Rüdiger, M. Gellert (Potsdam),

**R. Hollerbach (Leeds), A. Gailitis (Riga),
E. Kaplan (Grenoble), O. Kirillov (Moscow)**



The Yin-Yang of cosmical MHD



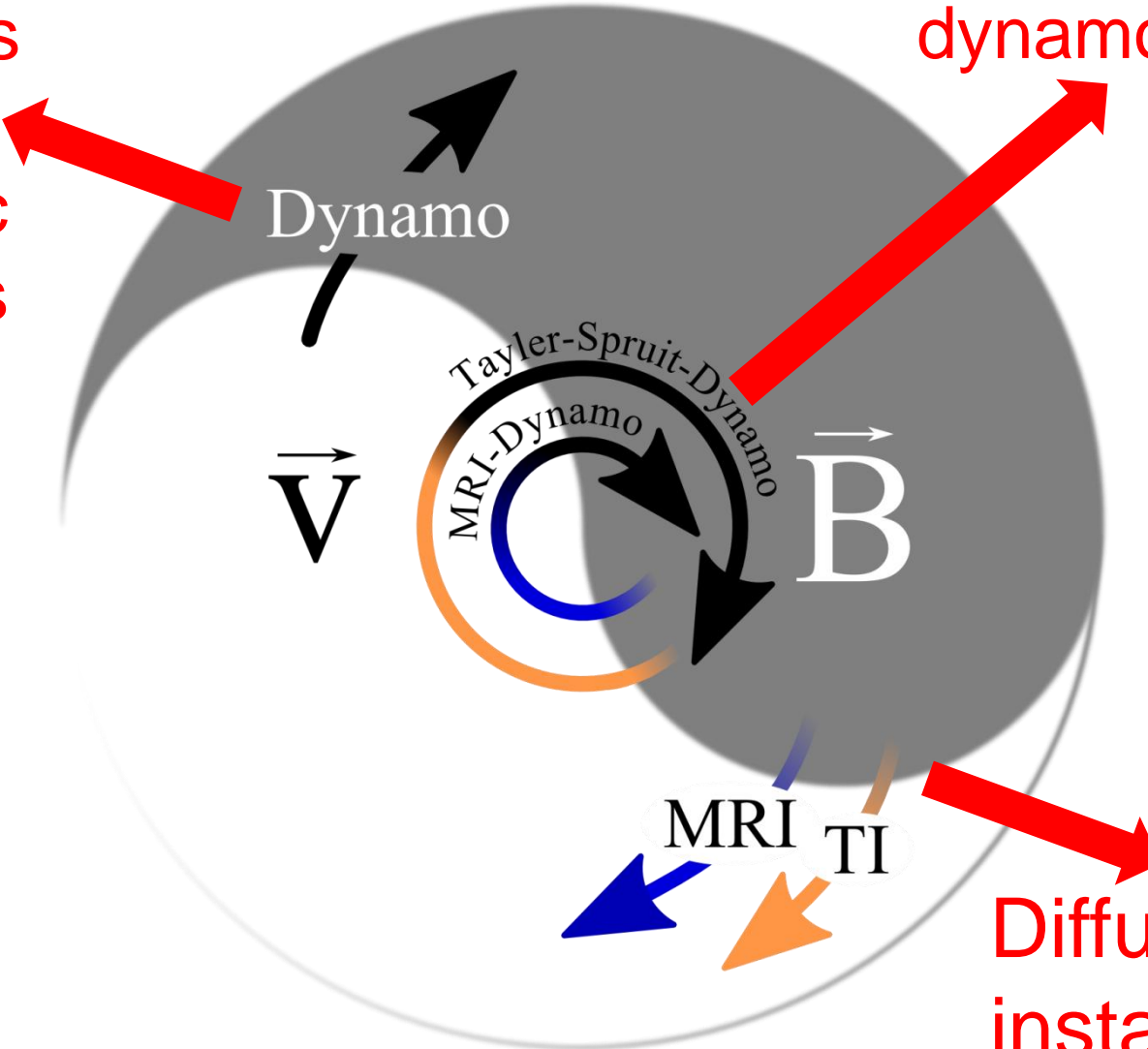
The Yin-Yang of cosmical MHD

Dynamos
with
magnetic
materials

Reversal
theory

Synchronized
dynamos

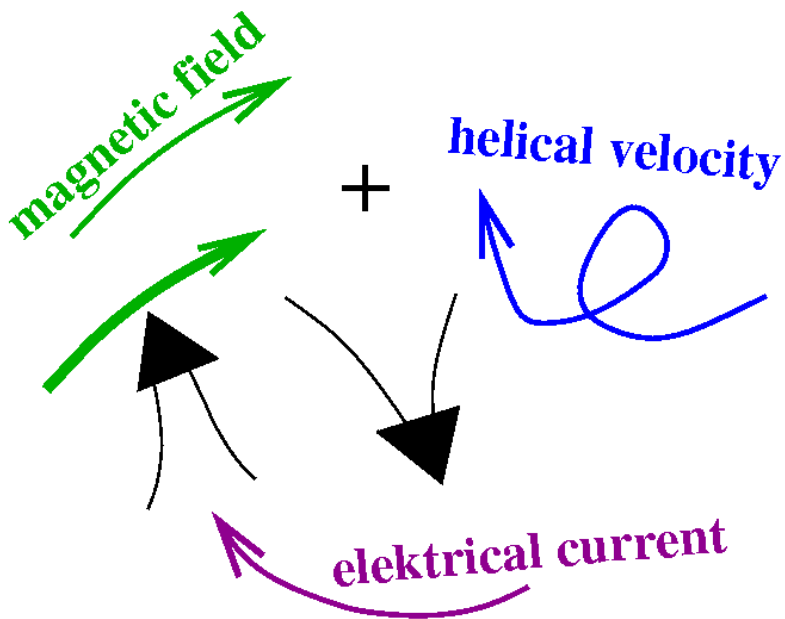
Diffusive
instabilities



Motivation

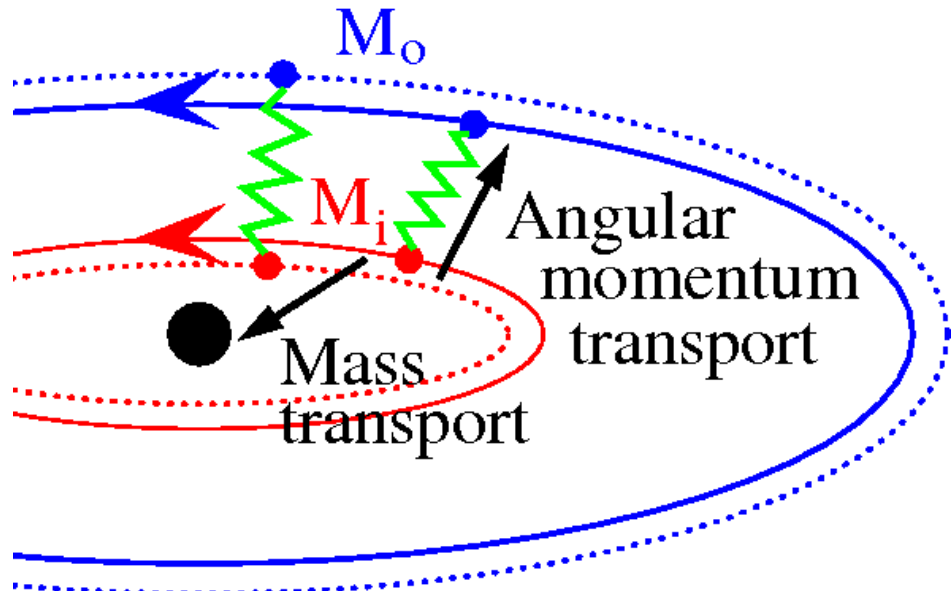
Homogeneous dynamo effect:

Self-excitation of magnetic fields in sufficiently strong, helical flows of conducting fluids

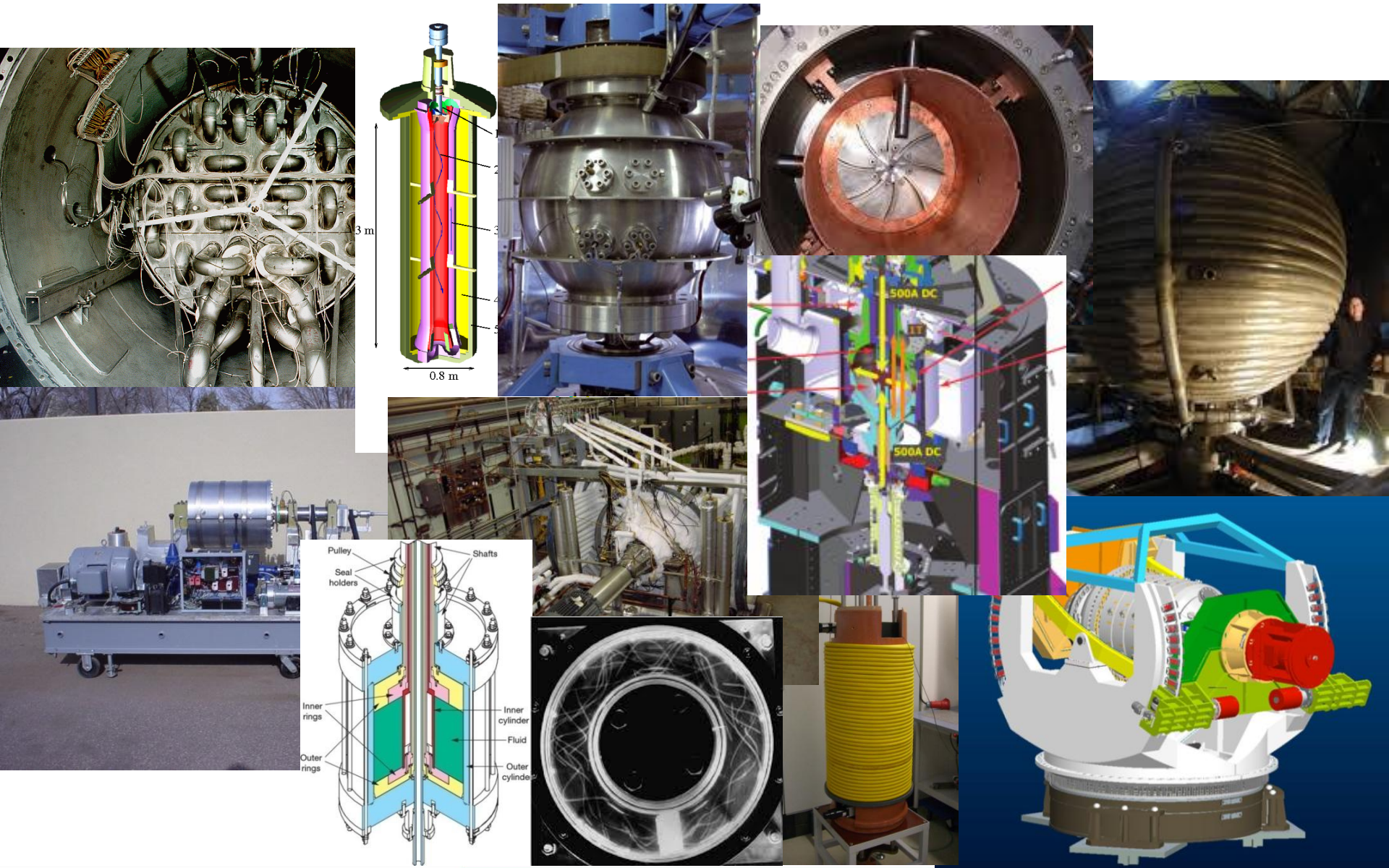


Magnetorotational instability (MRI):

Magnetic fields act like springs and trigger angular momentum transport in accretion disks around protostars and black holes



Previous, present, and future experiments



Prospects: DRESdyn

The *DREsden Sodium facility for DYNamo and thermohydraulic studies* → **platform for geo- and astrophysics experiments** as well as for liquid metal applications in energy related technologies.

- Precession driven dynamo experiment
- Magnetorotational instability (MRI) and Tayler instability (TI)
- Liquid metal batteries (storage of intermittent renewables)
- Measuring techniques (magnetic flow tomography etc...)
- Thermohydraulics of sodium fast reactors
- Large Rayleigh-Bénard (rotating?, magnetic field?) ???

Stefani et al.: Magnetohydrodynamics 48 (2012), 103;
Magnetohydrodynamics (2015), 51 (2015), 275



DRESDYN: General features

- New building ~500 m²
- Total sodium inventory: 12 tons
- Large experimental hall for **MRI/TI experiment**, sodium loop, X-ray lab, liquid metal batteries, Rayleigh-Bénard ?
- **Precession driven dynamo experiment** with separate strong basement and containment for Argon flooding



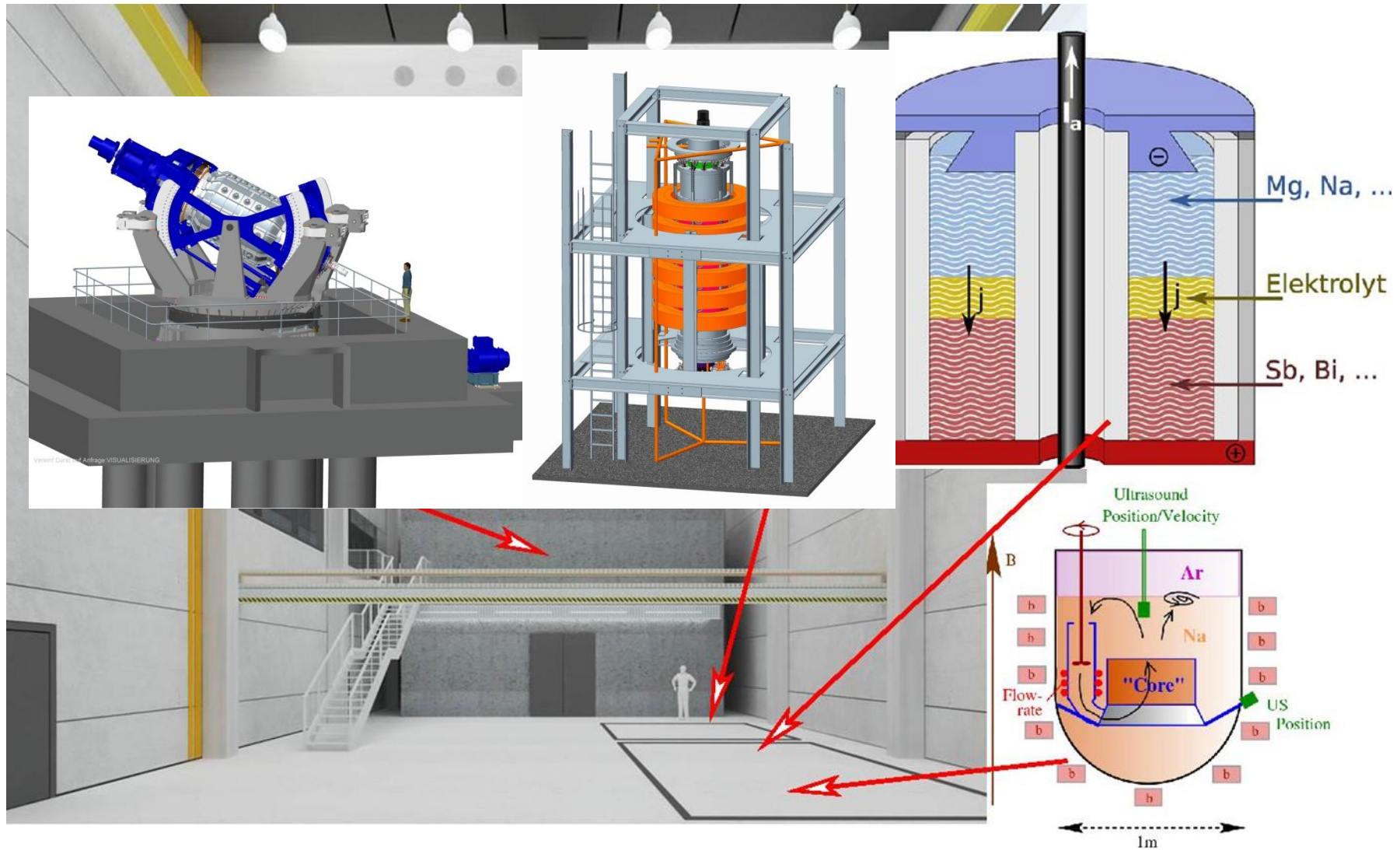
DRESDYN building as of January 2016: READY

DRESDYN: General features

- First sodium tank (of 4) has arrived (September 2016)

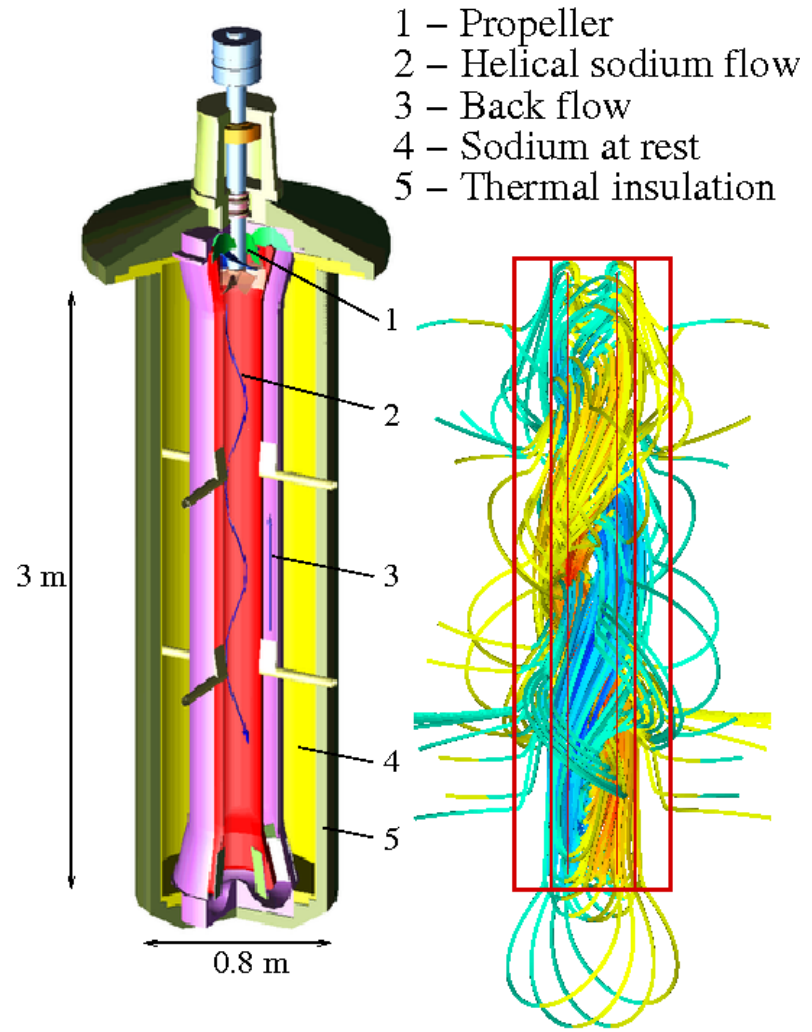


DRESDYN: General scheme



Dynamics

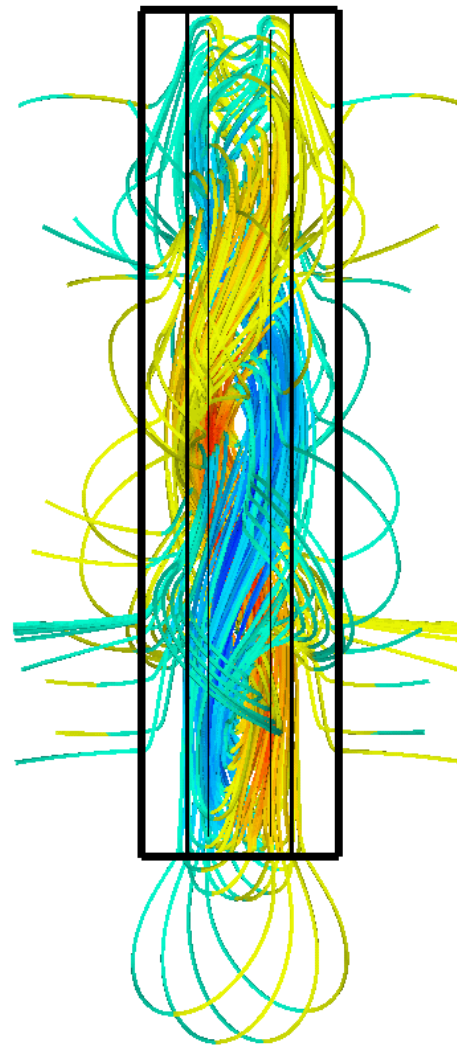
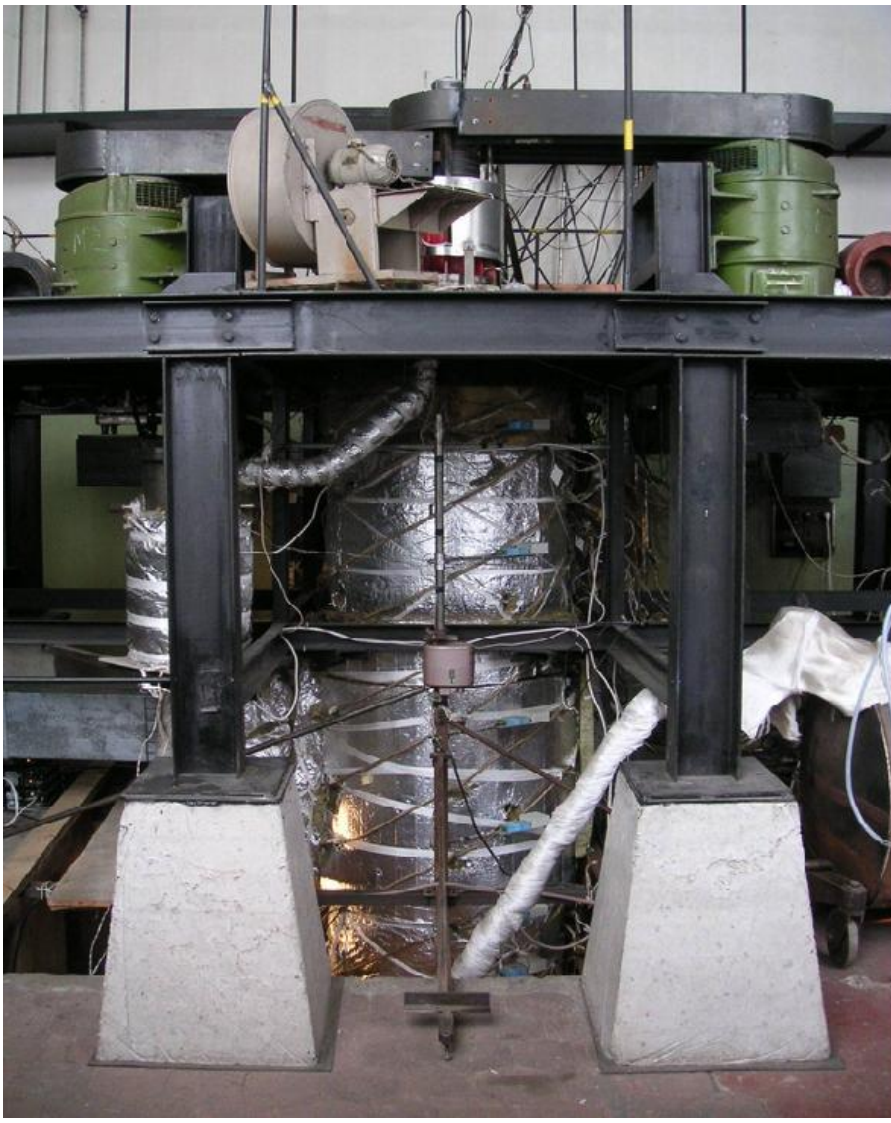
Riga dynamo experiment



Dynamo
module

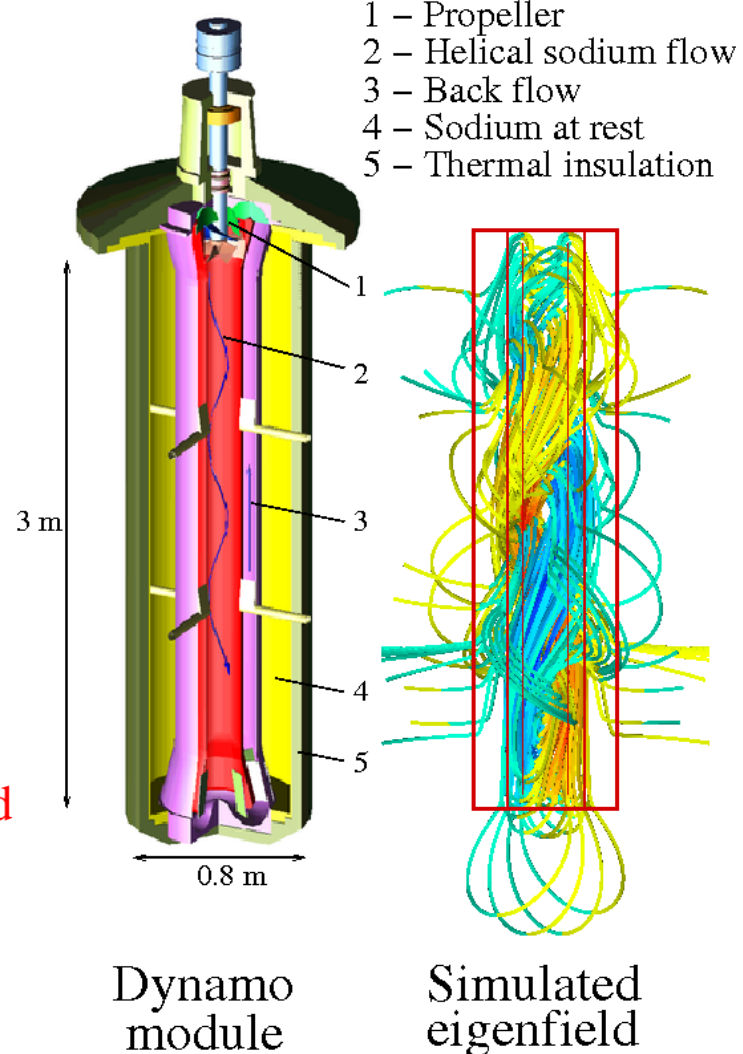
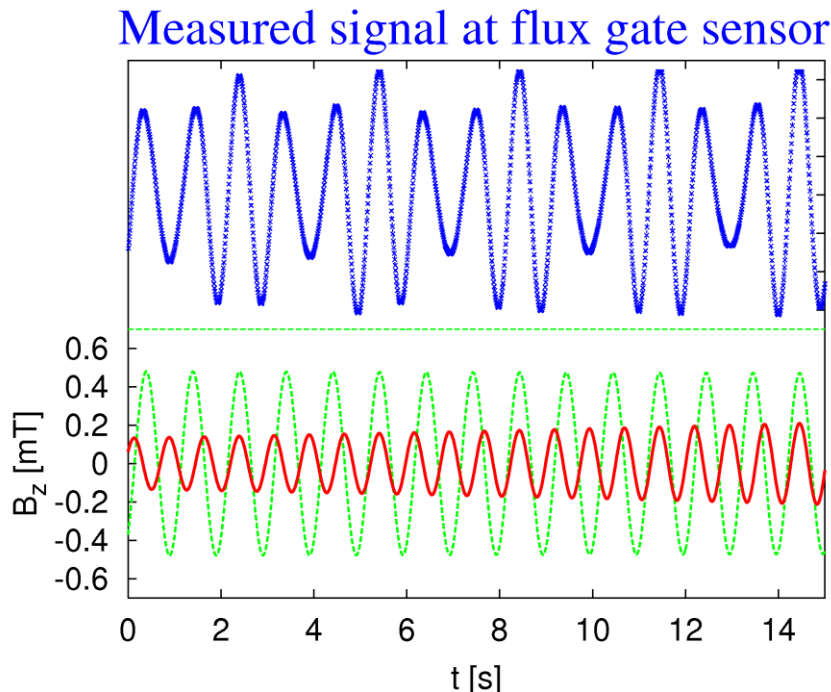
Simulated
eigenfield

Riga dynamo experiment



Riga dynamo experiment

First experimental realization of magnetic field self-excitation in a liquid metal flow
(11 November 1999)



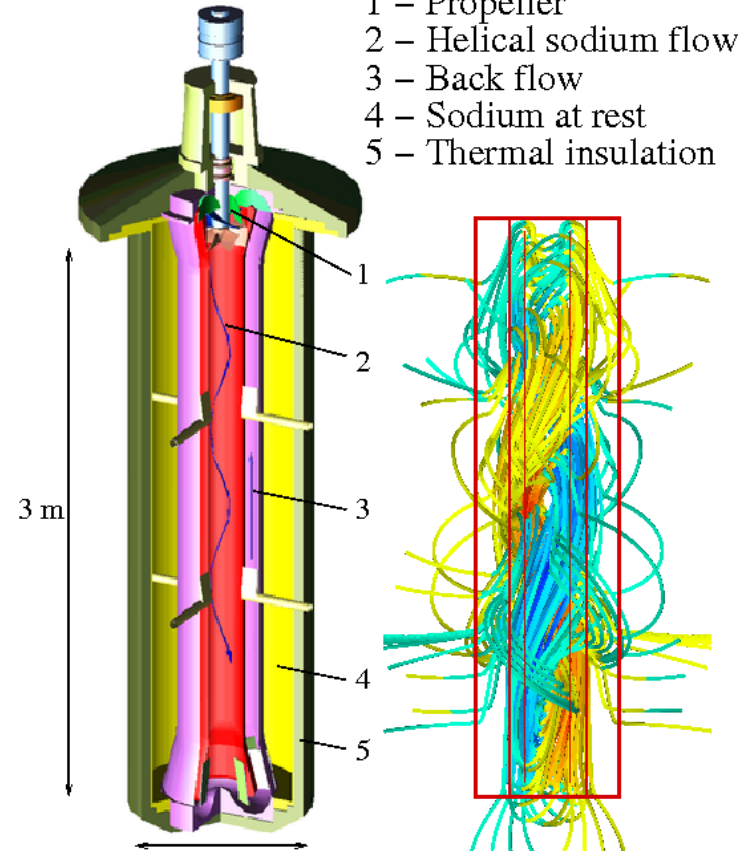
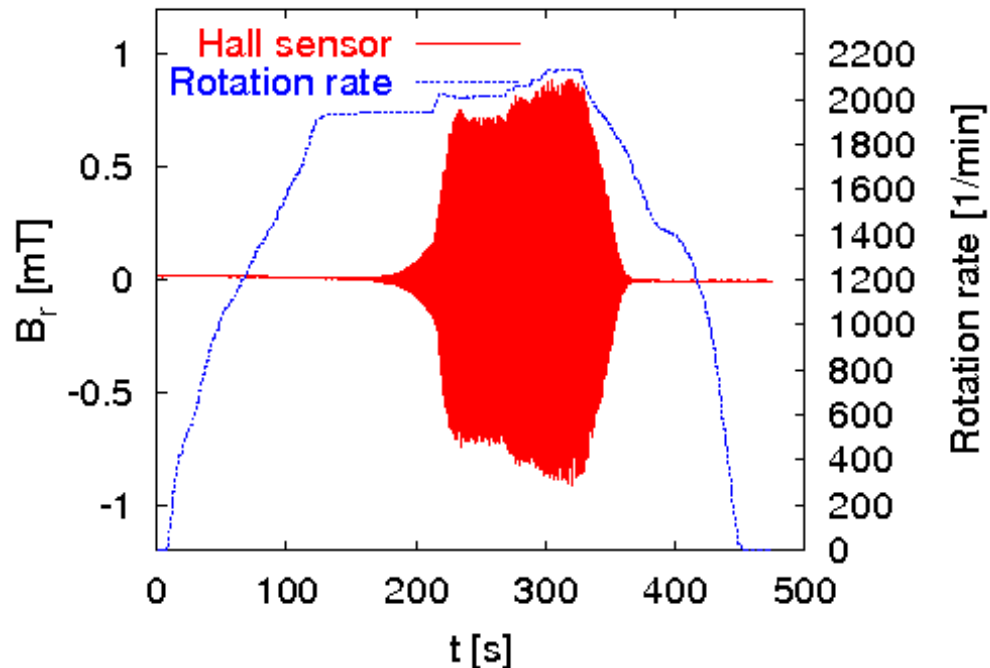
Dynamo module

Simulated eigenfield

Gailitis et al., Phys. Rev. Lett. 84 (2000) 4365; Phys. Rev. Lett. 86 (2001) 3024; Rev. Mod. Phys. 74 (2002) 973 ; Phys. Plasmas 11 (2004) 2838; Compt. Rend. Phys. 9 (2008), 721

Riga dynamo experiment

From the kinematic to the saturated regime (July 2000)



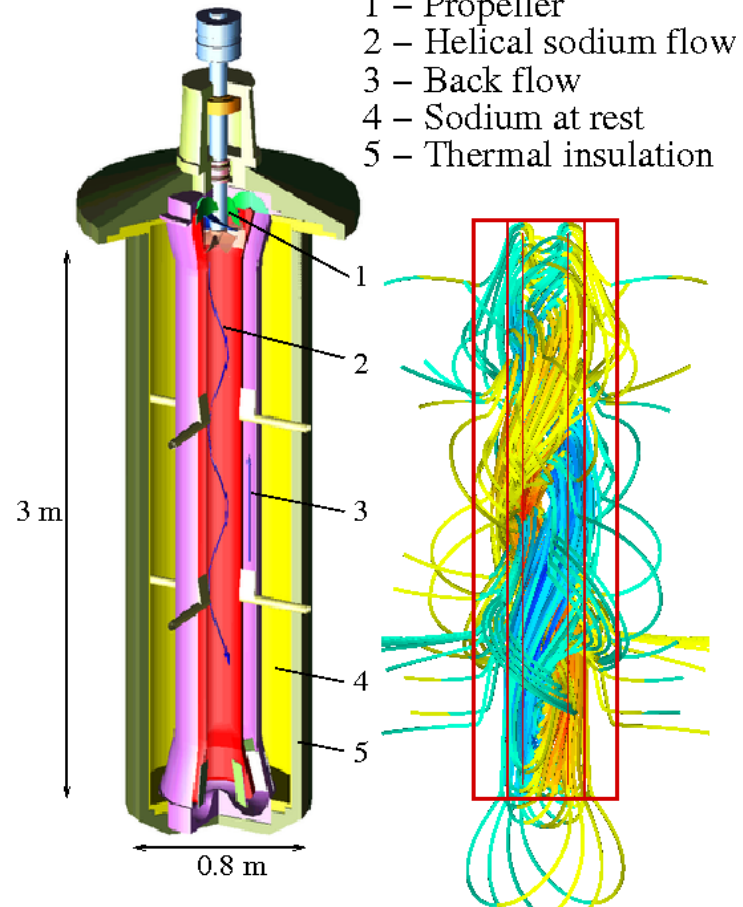
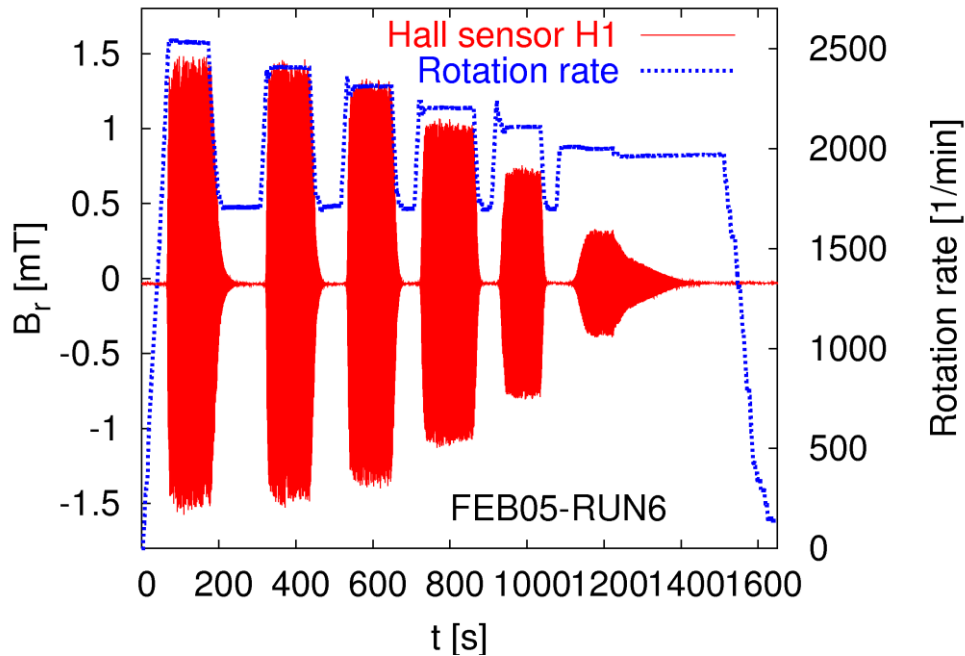
Dynamo
module

Simulated
eigenfield

Gailitis et al., Phys. Rev. Lett. 84 (2000) 4365; Phys. Rev. Lett. 86 (2001) 3024; Rev. Mod. Phys. 74 (2002) 973 ; Phys. Plasmas 11 (2004) 2838; Compt. Rend. Phys. 9 (2008), 721

Riga dynamo experiment

Switching the dynamo on and off
(February 2005)

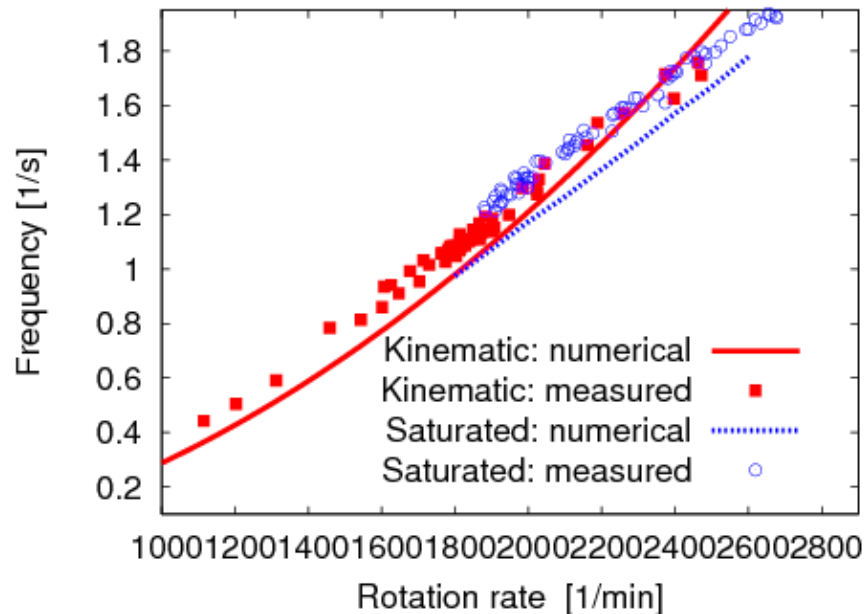
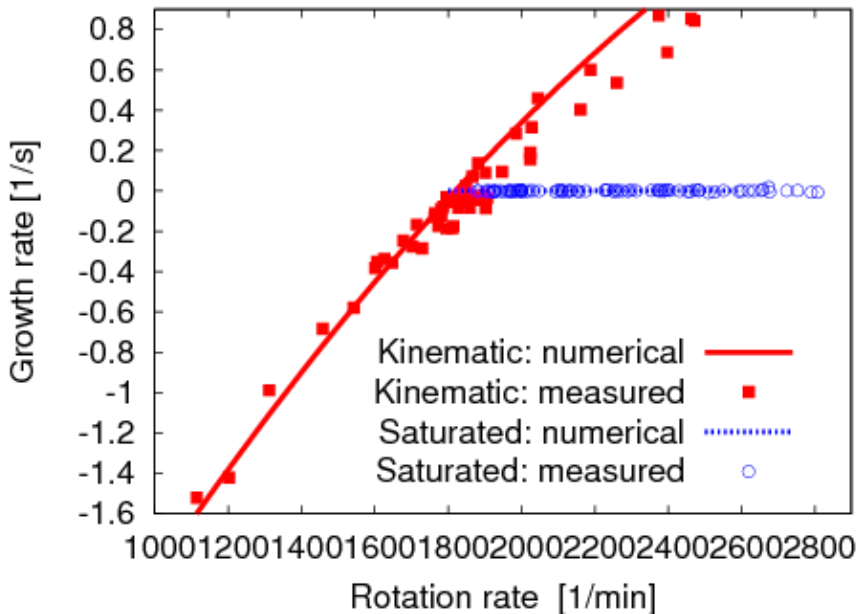


Dynamo module

Simulated eigenfield

Gailitis et al., Phys. Rev. Lett. 84 (2000) 4365; Phys. Rev. Lett. 86 (2001) 3024; Rev. Mod. Phys. 74 (2002) 973 ; Phys. Plasmas 11 (2004) 2838; Compt. Rend. Phys. 9 (2008), 721

Riga dynamo experiment: Growth rates and frequencies



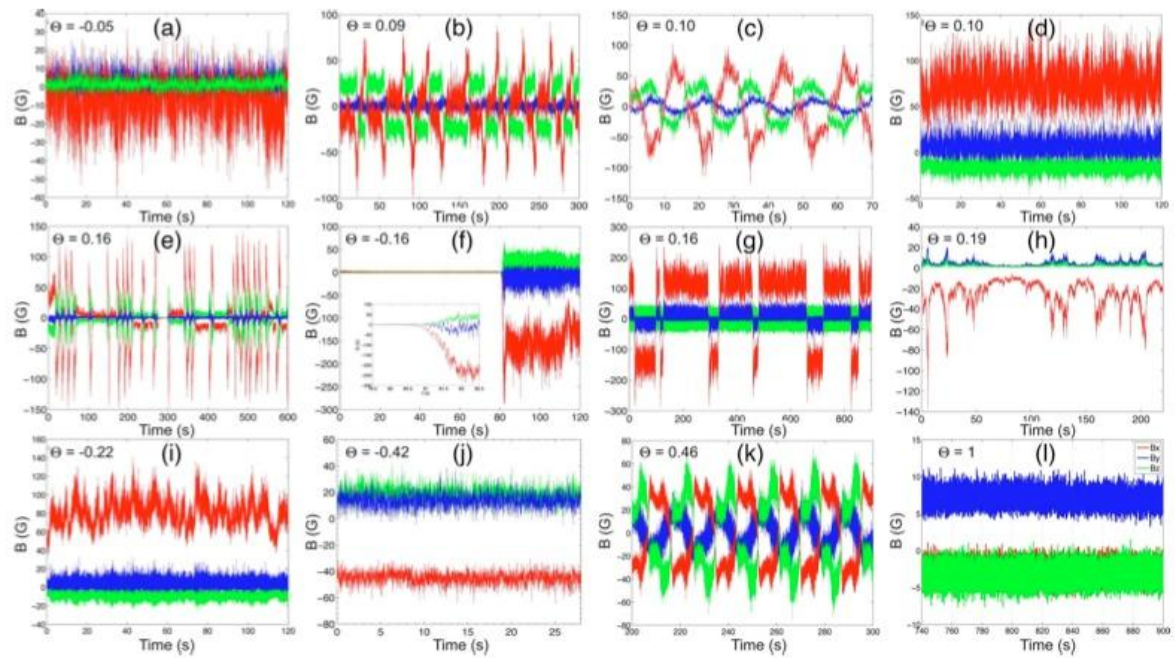
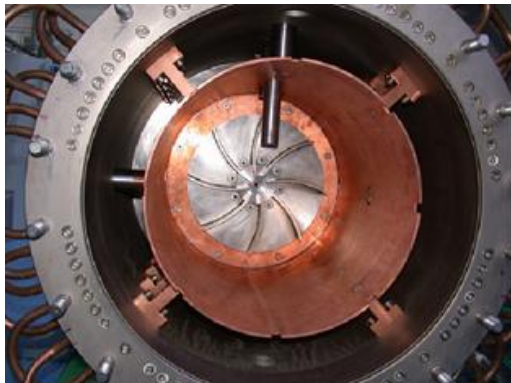
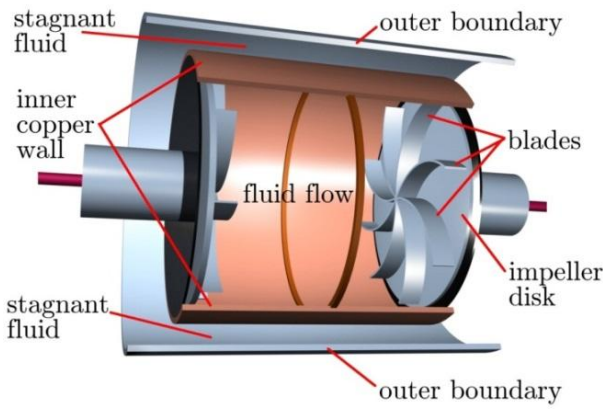
Numerical predictions (with correct vacuum boundary conditions) of the kinematic dynamo were accurate to some 5-10 per cent

Simplified back-reaction model (Lorentz forces acting along streamlines) gives very reasonable field amplitudes and structures in the saturation regime

Gailitis et al., C. R. Physique 9 (2008), 721

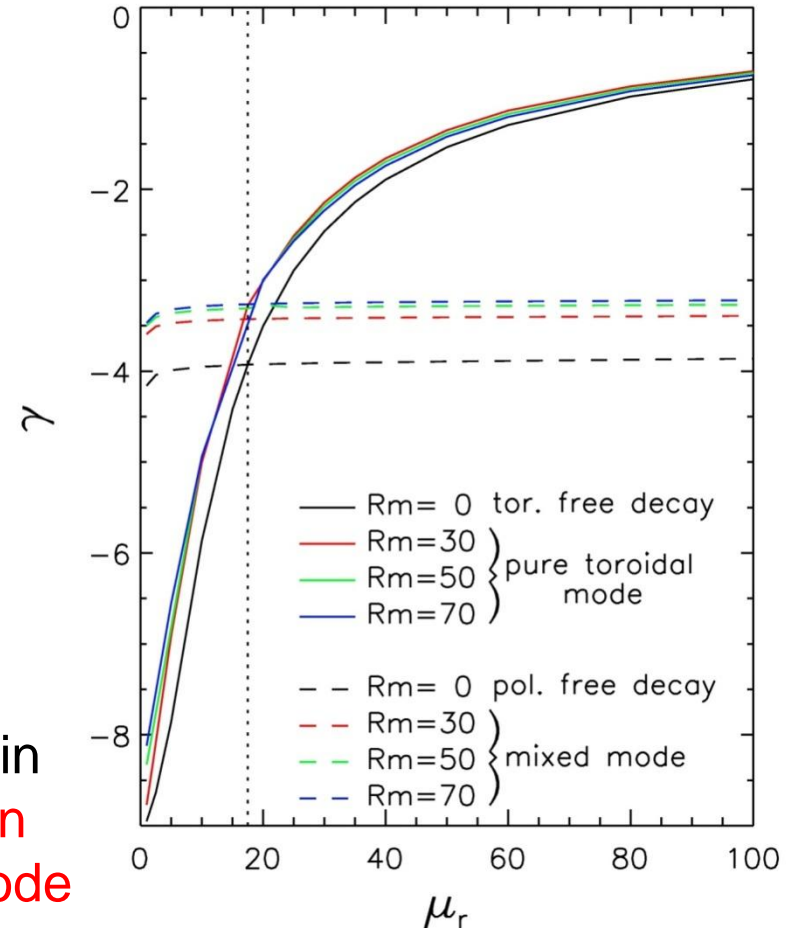
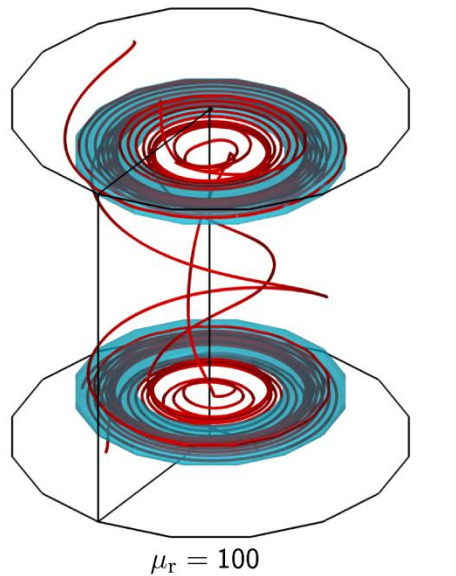
von-Karman-Sodium (VKS) Experiment

VKS has shown self-excitation and a wealth of wonderful dynamical effects, including **oscillations, reversals, burst, localized fields**....



Monchaux et al., Phys. Fluids 21, 035108 (2009)

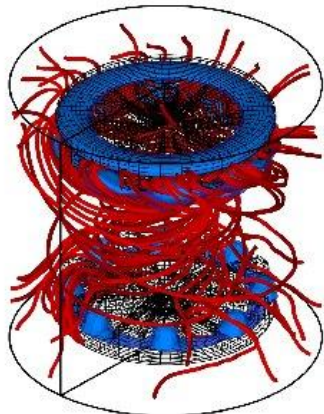
VKS-Dynamo: Role of high μ impellers?



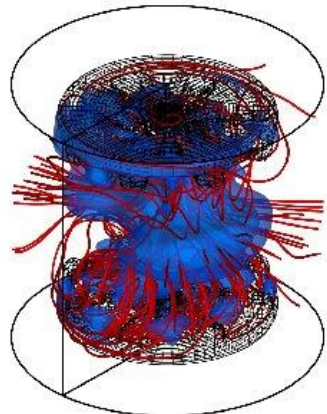
Crucial role of high μ_{rel} impellers, even in the free-decay case: **Transition between dominant poloidal and toroidal eigenmode at $\mu_{\text{rel}} \sim 20$**

Giesecke et al., GAFD 104 (2010); New J. Phys. 14 (2012)

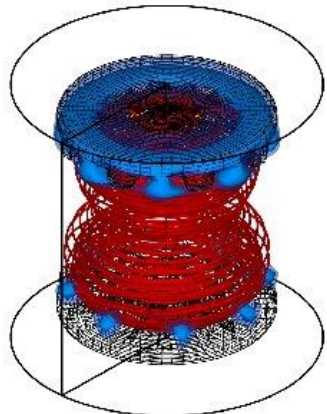
VKS-Dynamo: Role of high μ impellers?



(a)



(b)

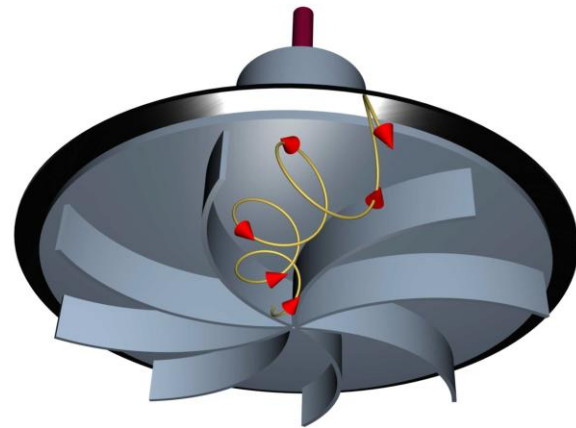
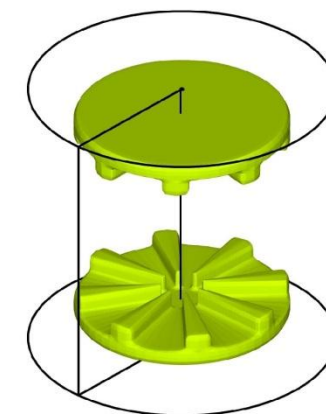


(c)

$Rm=30, \alpha=-1.5$
growing $m=0$

$Rm=70, \alpha=0$
growing $m=1$

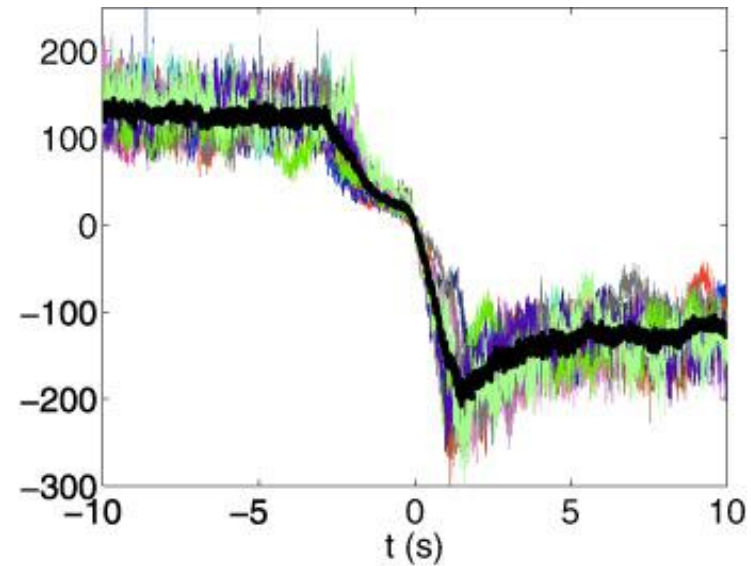
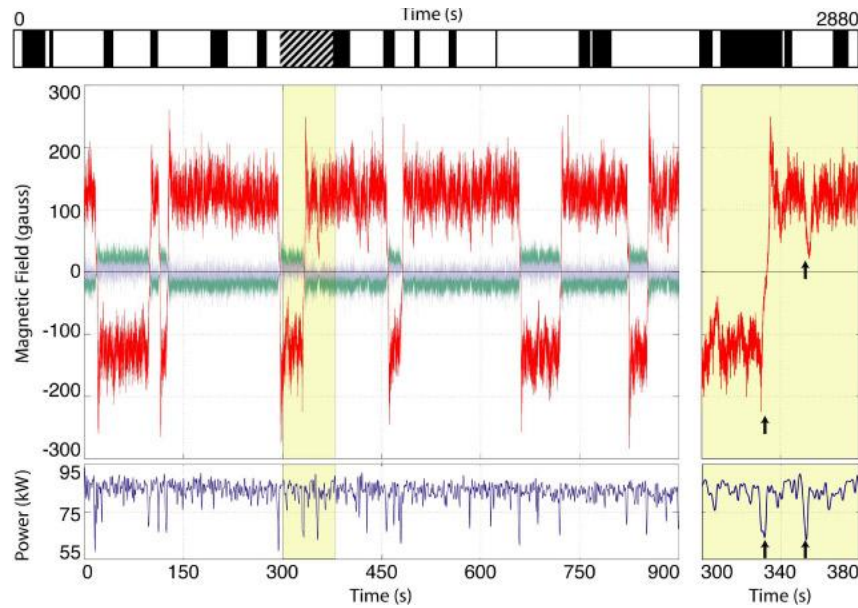
$Rm=30, \alpha=0$
decaying $m=0$



...on the basis of the dominant toroidal mode,
some small-scale helicity between the blades
(α -effect) is sufficient to ignite the dynamo

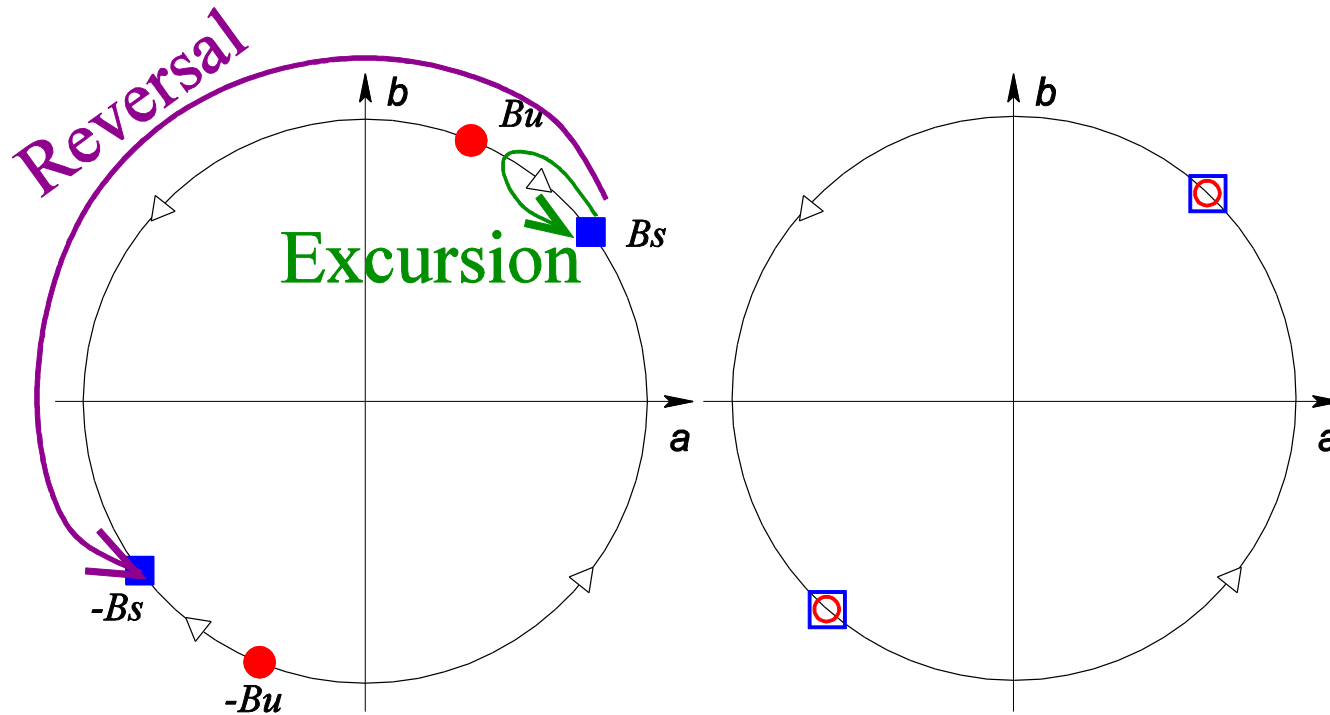
Giesecke et al., Phys. Rev. Lett. 104 (2010)

Reversals of the geomagnetic field and the VKS dynamo field



Berhanu et al., EPL 77 (2007), 59001

Reversals of the geomagnetic field and the VKS dynamo field

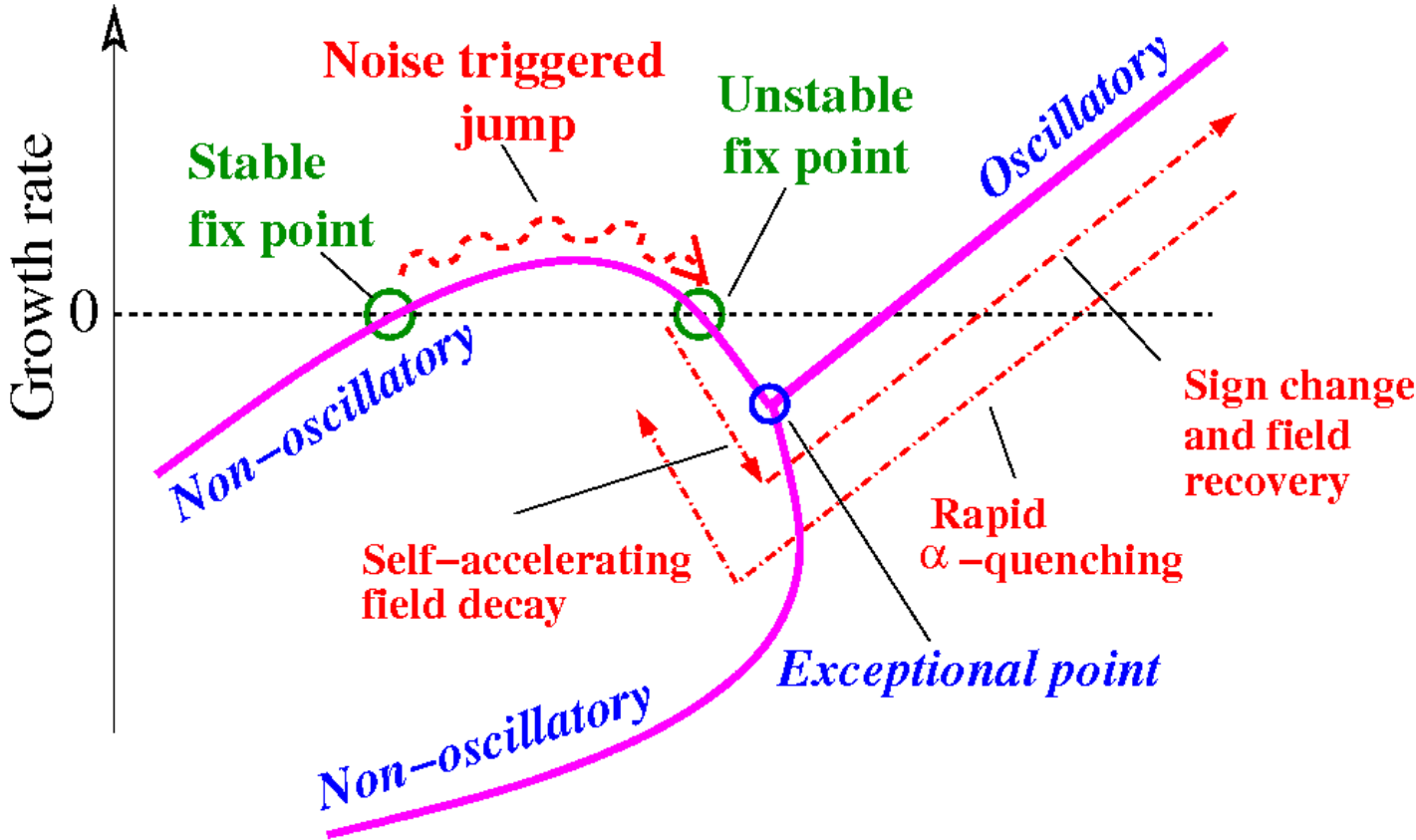


Dynamical systems
approach: Saddle-
node bifurcation

$$\frac{d\Theta}{dt} = \alpha_0 + \alpha_1 \sin(2\Theta) + \text{noise}$$

Petrelis et al., PRL 102 (2009), 144503

Reversals of the geomagnetic field and the VKS dynamo field

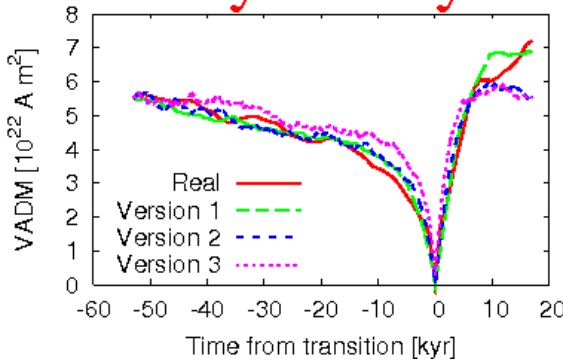


Spectral properties of a (spherically symmetric) α^2 dynamo

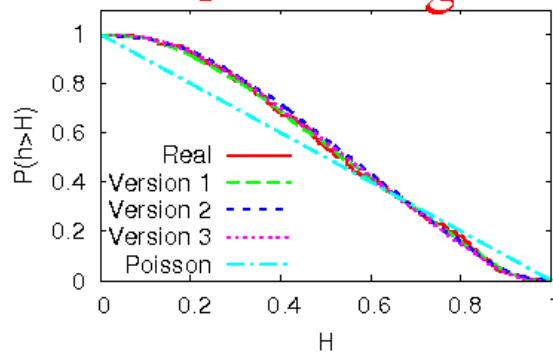
Stefani et al., PRL 94 (2005) 184506; Earth Planet. Sci.Lett. 243 (2006), 828; GAFD 101 (2007) 227; Fischer et al., Inverse Probl. 25 (2008) 065011

Reversals of the geomagnetic field and the VKS dynamo field

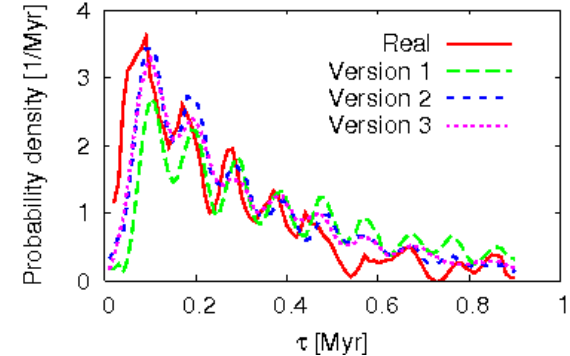
Asymmetry



Clustering



Stochastic resonance



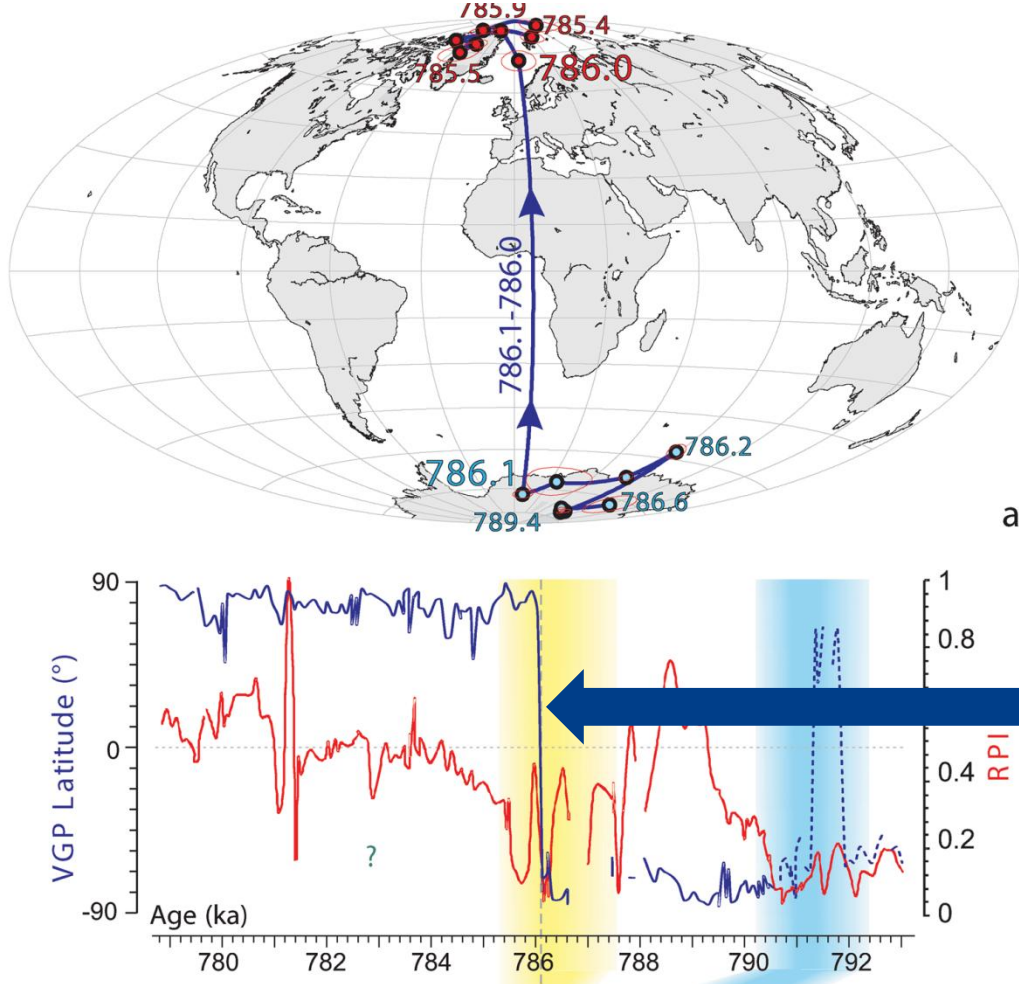
Simple model explains many features of reversals, and can be used to constrain basic parameters of the geodynamo. Best results for:

- Supercriticality of the dynamo: Factor 10
- Relative strength of periodic forcing: 10 per cent
- Diffusion time: 64 kyr, i.e **reduction by a factor 3.5** compared to 225 kyr from molecular conductivity. This is in rough agreement with numerical simulations (Schriener et al. 2007) and **β effect measured in Perm** .

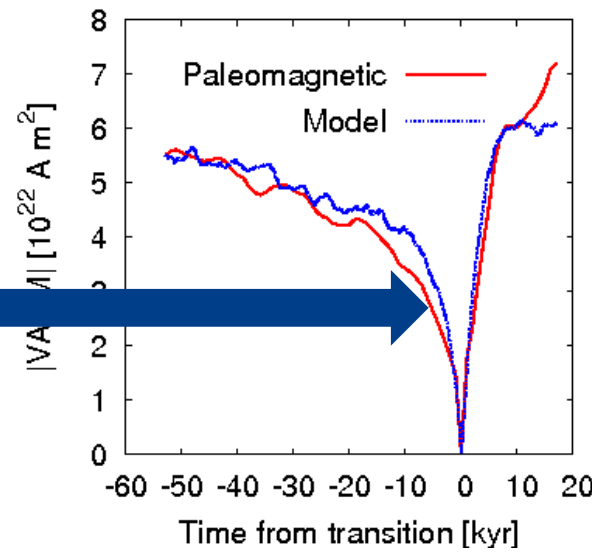
Fischer et al., Inverse Probl. 25 (2008) 065011

Reversals of the geomagnetic field and the VKS dynamo field

Further dynamo constraints may follow from the recent observation of very fast reversals



Sagnotti et al., Geophys.J.Int. 199
(2014), 1110

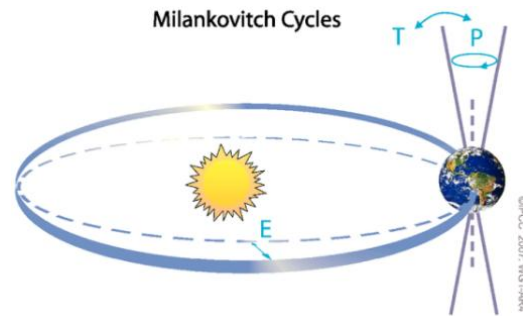
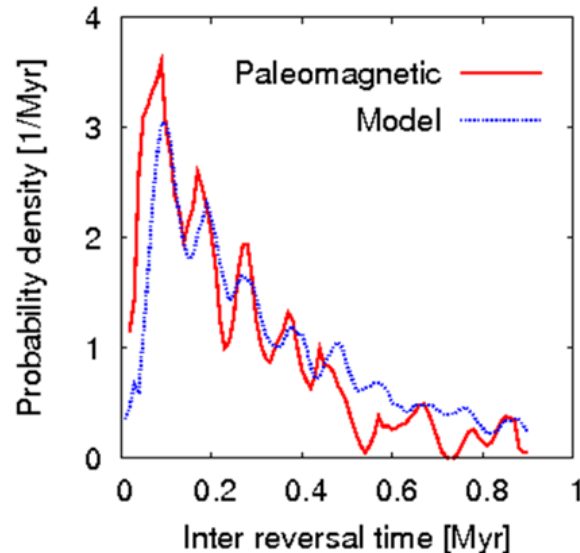


Summary on Reversals

- Reversals are (very likely...) noise triggered relaxation oscillations in the vicinity of exceptional points of the spectrum of the dynamo operator \longleftrightarrow in the parlance of dynamical systems, this corresponds to a saddle-node bifurcation
- Highly supercritical dynamos tend to self-tune into a reversal-prone state ("edge of chaos", "self-organized criticality" ???)
- Asymmetry, clustering, and stochastic resonance can be used as proxies for constraining essential parameters of the geodynamo.
- The estimated conductivity reduction, if anisotropic, would be important for dynamo simulations (selection of axial or equatorial dipole, etc.)

The DRESDYN precession dynamo: Geo/astrophysical motivation

Strong indication for influence of variations of Earth's orbit parameters on the geodynamo



Probability density of inter-reversal times shows maxima at multiples of the Milankovic cycle of Earth's orbit eccentricity (95 ka) \longleftrightarrow climate??

Consolini and De Michelis, Phys. Rev. Lett.
90 (2003), 058503

Recent discussion of the **lunar dynamo** in terms of precession or impacts

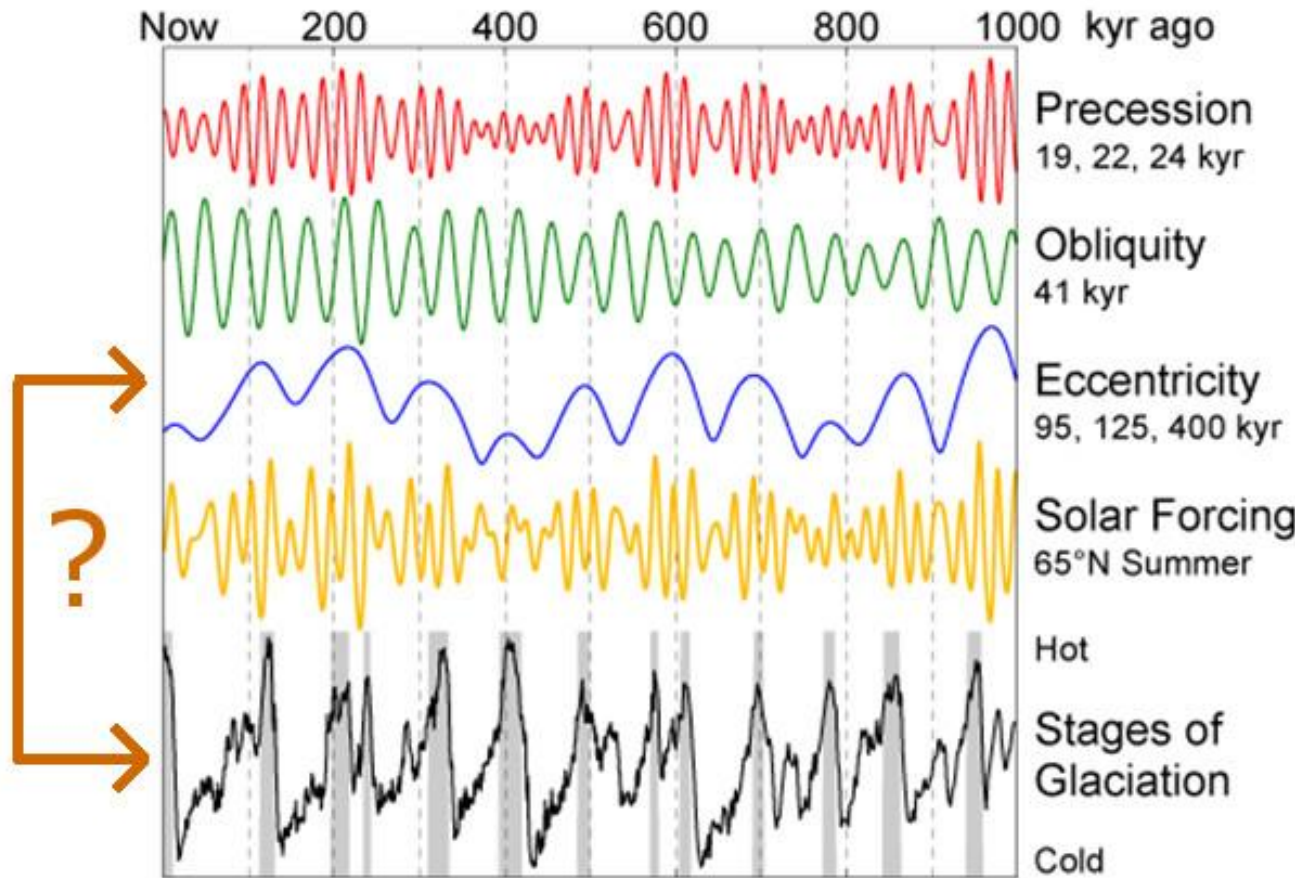
Dwyer et al., Nature 479 (2011), 212; Le Bars et al., Nature 479 (2011), 215

Evidence for ancient core **dynamo** in asteroid Vesta

Fu et al., Science 338 (2012), 238

The DRESDYN precession dynamo: Geophysical motivation

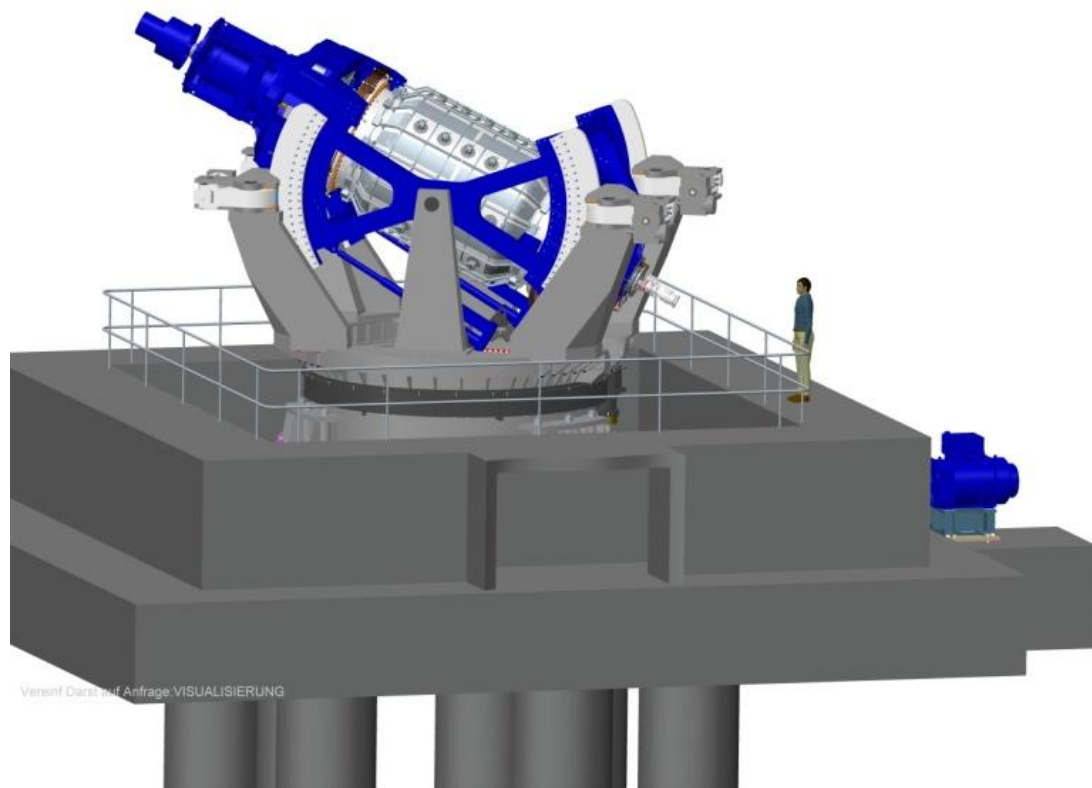
**Most interesting connection between geomagnetic field and climate
(sequence of ice ages)**



Precession driven dynamo: Experiment is designed and (partly) under construction

Key parameters:

- 2 m diameter, 2 m height,
8 m³ liquid sodium
- Cylinder rotation: 10 Hz
(will need some 800 kW
motor power)
- Turntable rotation: 1 Hz
- **Magnetic Reynolds**
number ~ 700
- Gyroscopic **torque onto**
the basement: 8 MNm !



Vereinf. Darst. auf Anfrage: VISUALISIERUNG

“Fundamental” problems due to huge gyroscopic torque

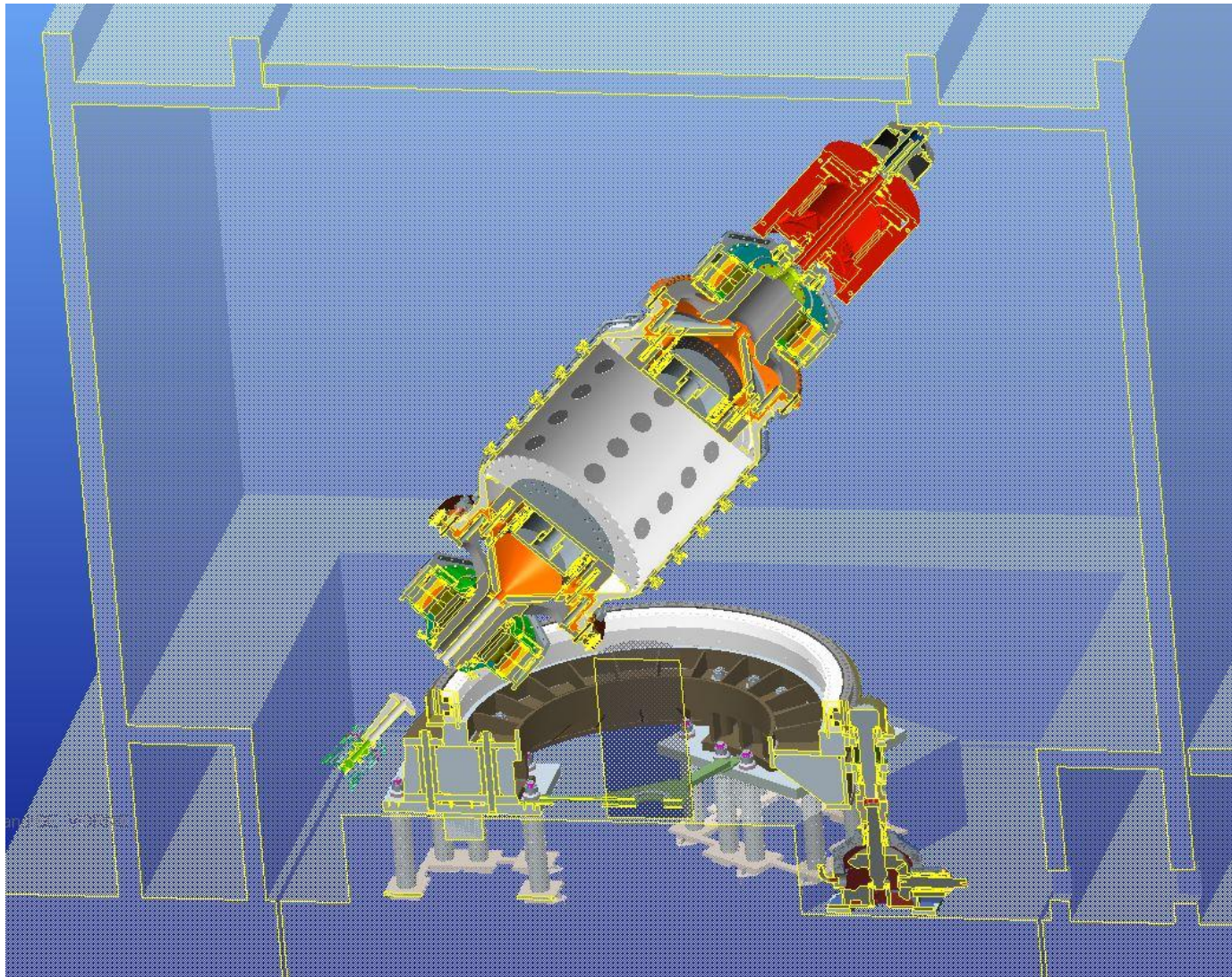
April 2013: drilling 7 holes (22 m deep)



July 2013: Constructing the ferroconcrete basement

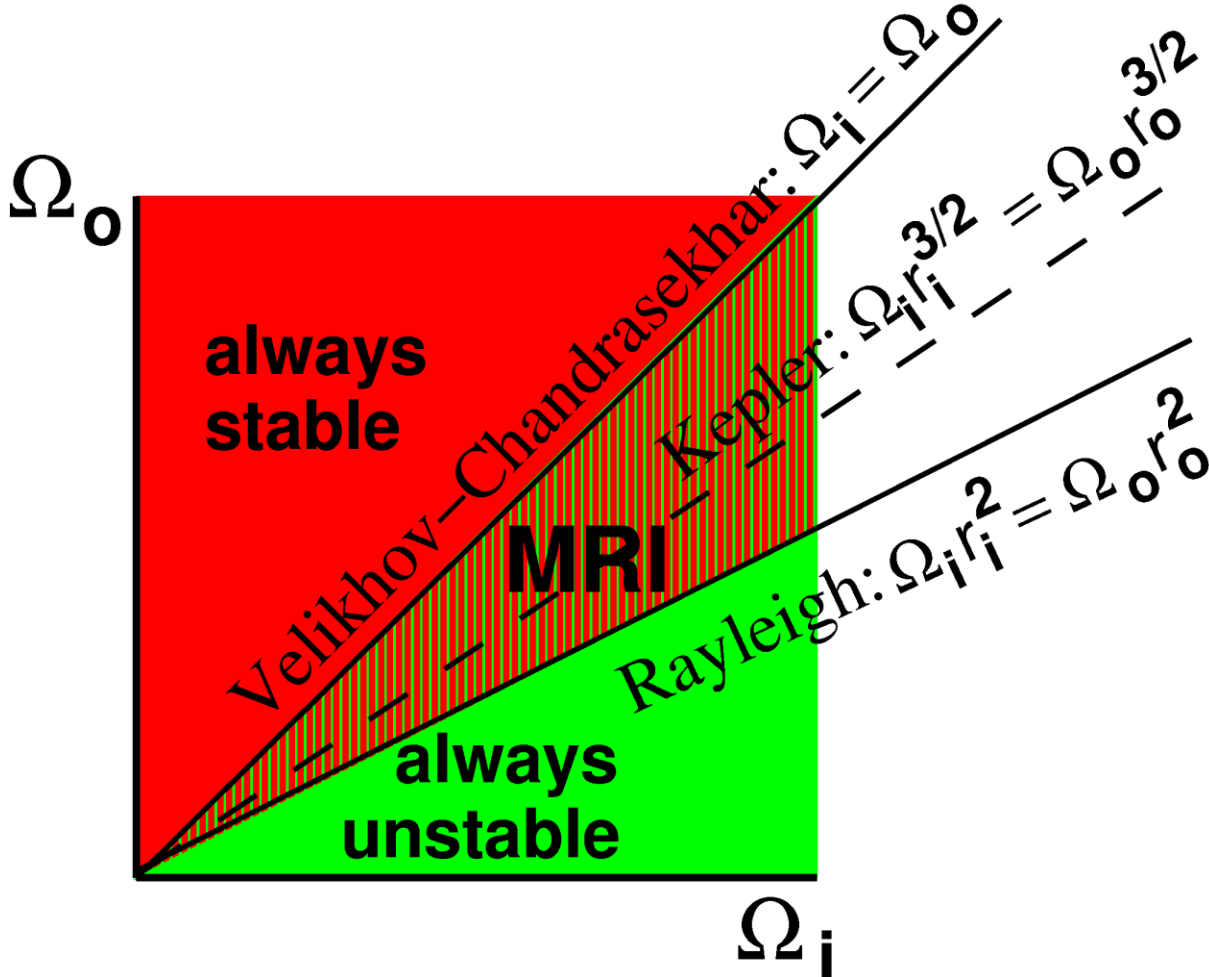
May 2015: The tripod for the dynamo within the containment (with stainless steel “wallpaper”)

Precession driven dynamo: Situation in the containment



Magnetorotational and Tayler instability

History of MRI: Magnetized Tayler-Couette flow



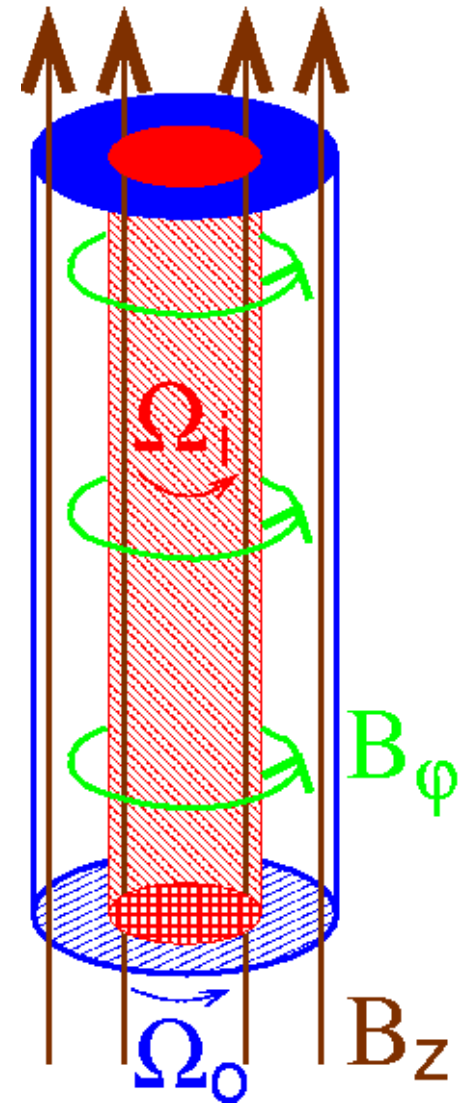
E.P. Velikhov: Sov. Phys. JETP 9 (1959), 995

Standard MRI and helical MRI

- Standard MRI (with purely axial field) scales with Lundquist (S) und magnetic Reynolds (Rm)
- Experiments on SMRI with large Rm in Maryland and Princeton → DRESDYN
- Helical MRI: B_z replaced by $B_z + B_\phi$: scales with Hartmann (Ha) and Reynolds (Re)

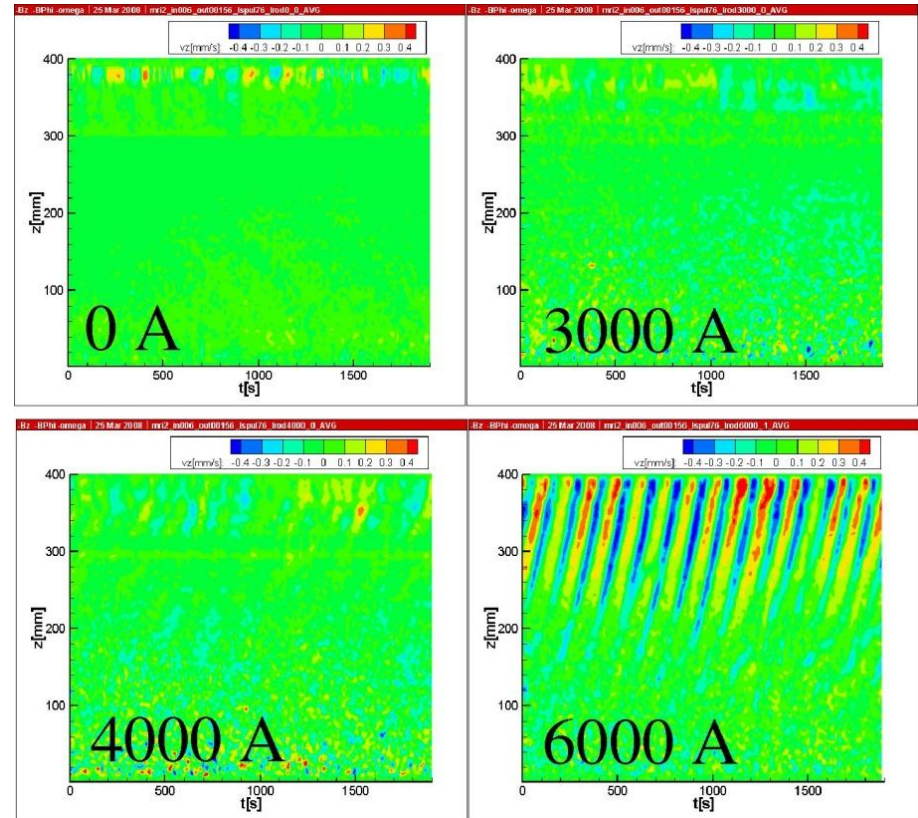
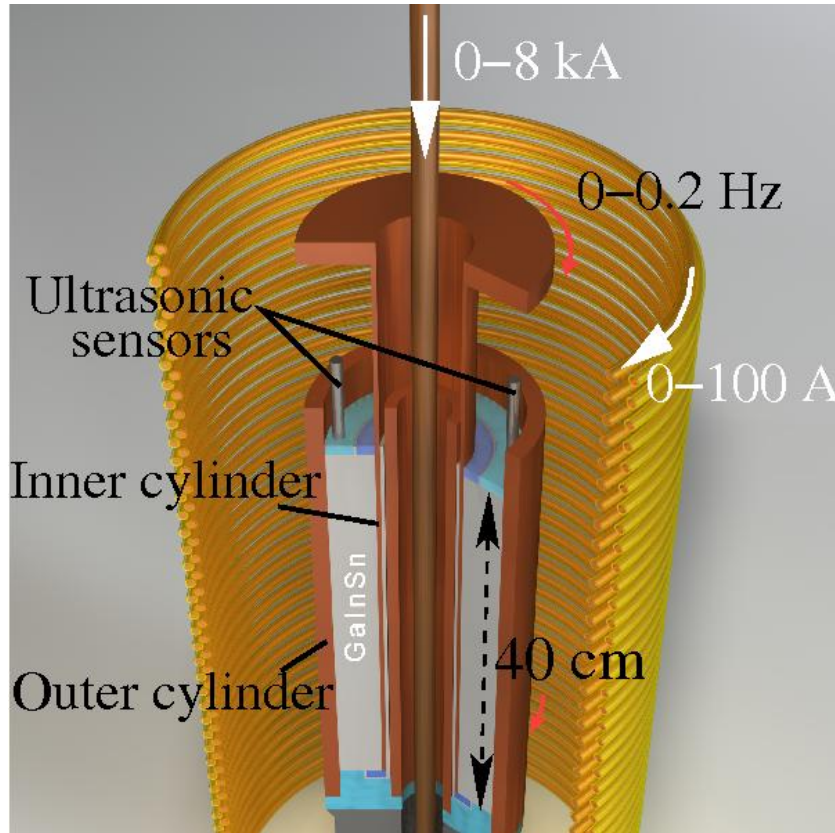
Hollerbach and Rüdiger: Phys. Rev. Lett. 95 (2005), 124501

- Re_{crit} : 10^3 instead of 10^6
- Ha_{crit} : 30 instead of 1000
- → Potsdam ROssendorf Magnetic InStability Experiment (PROMISE)
- Drawback: does not work for Kepler (yet)!



Helical magnetorotational instability (HMRI)

2006: First experimental evidence of HMRI

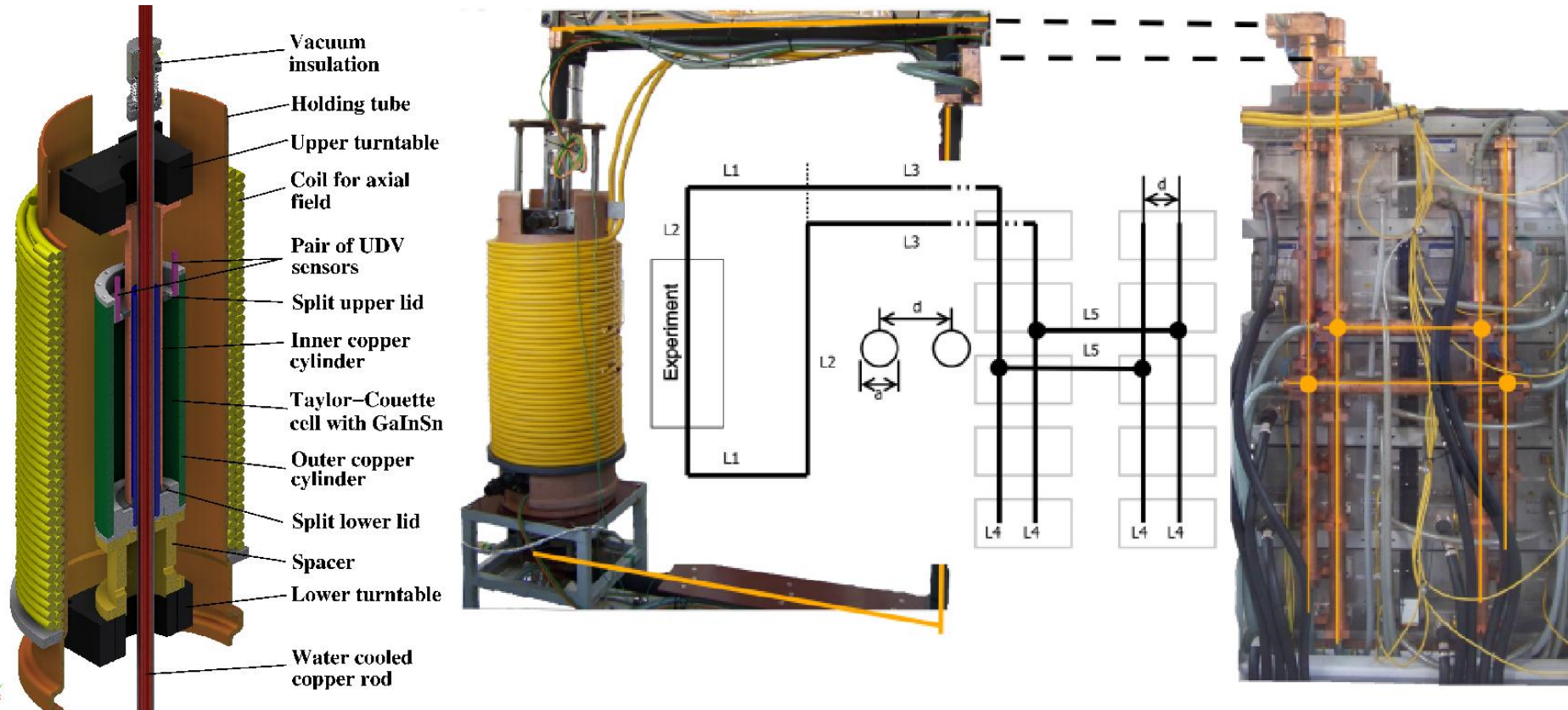


Stefani et al., Phys. Rev. Lett. 97 (2006), 184502; New J. Phys. 9 (2007), 295; Phys. Rev. E 80 (2009), 066303

Azimuthal MRI (AMRI): $m=1$ mode under influence of dominant B_ϕ

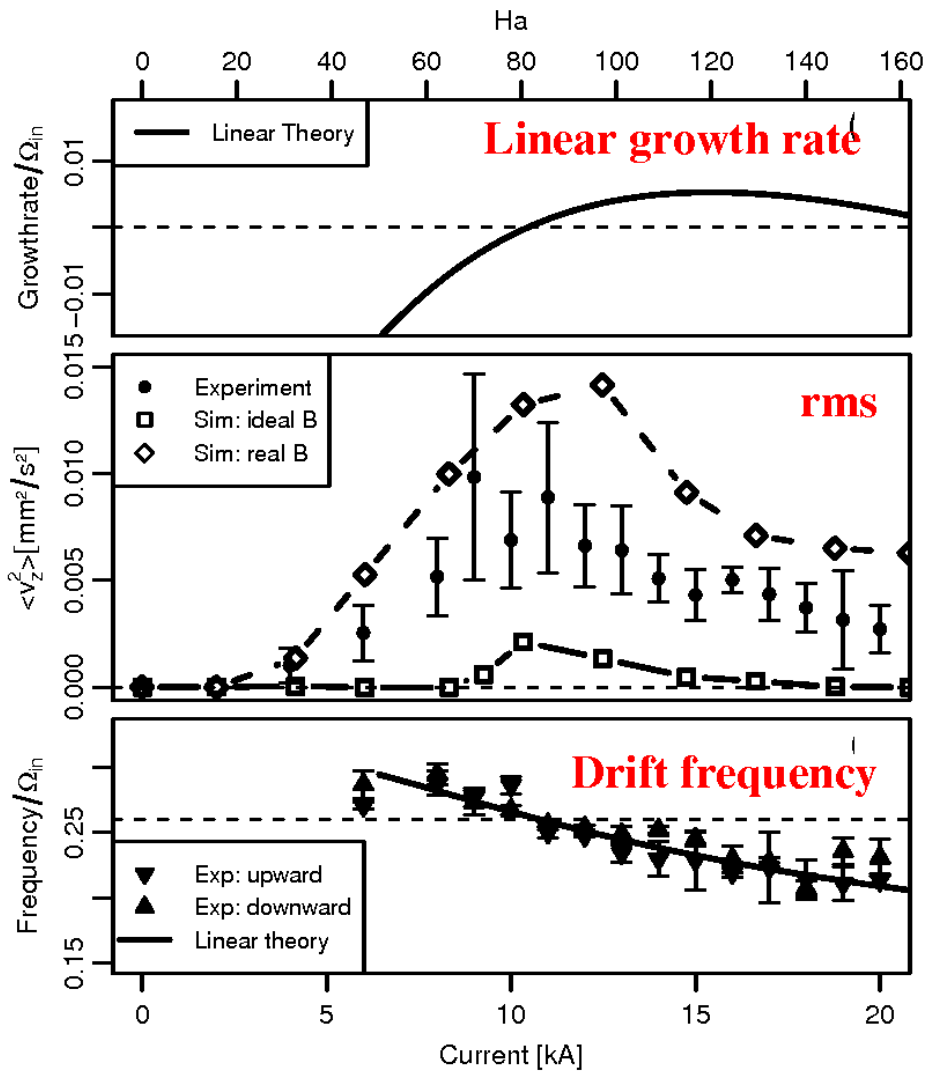
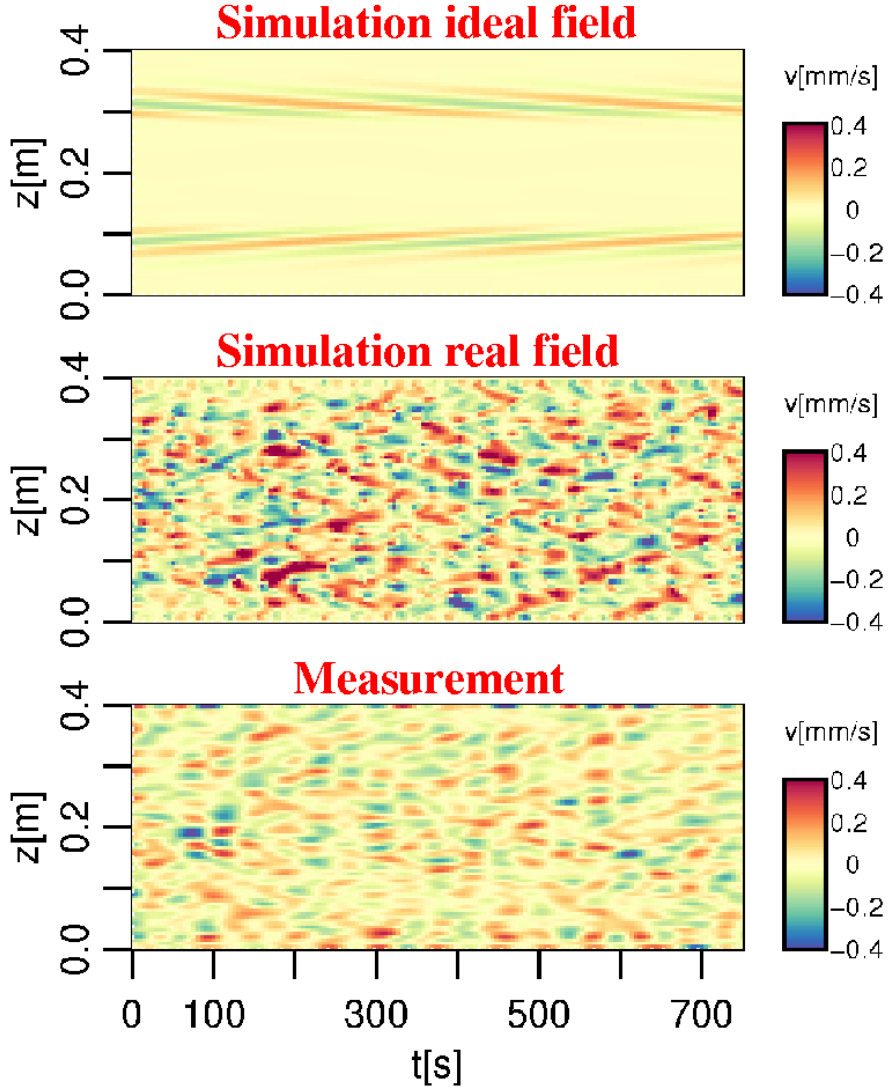
Hollerbach, Teeluck, Rüdiger:
Phys. Rev. Lett. 104 (2010), 044502

New power supply for 20 kA



Very important: Numerical simulation of the real geometry, including the slight symmetry breaking of the applied magnetic field

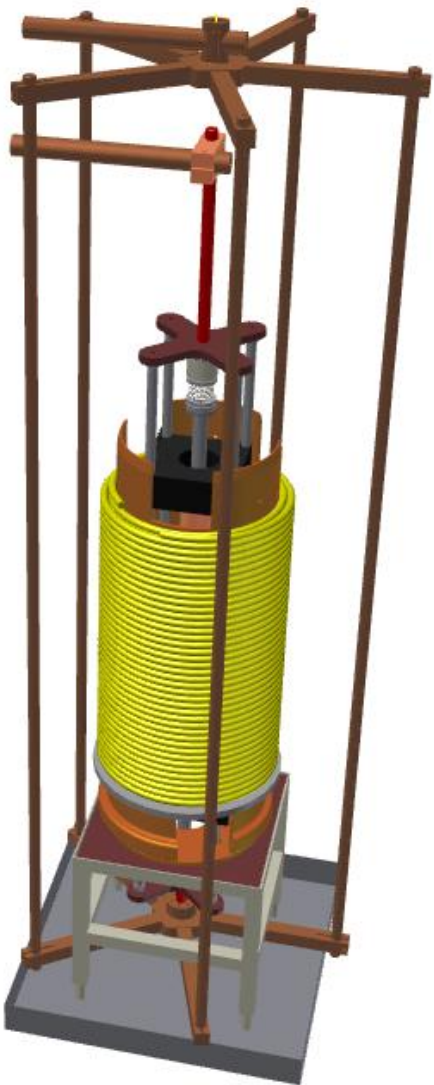
Evidence for AMRI: $m=1$ mode under influence of (nearly) pure B_ϕ



Seilmayer et al., Phys. Rev. Lett. 113 (2014), 024505

PROMISE 3: Improves the symmetry of the applied field

The symmetry of the field can be strongly enhanced by a cage-like structure of the return-current with n “wires”



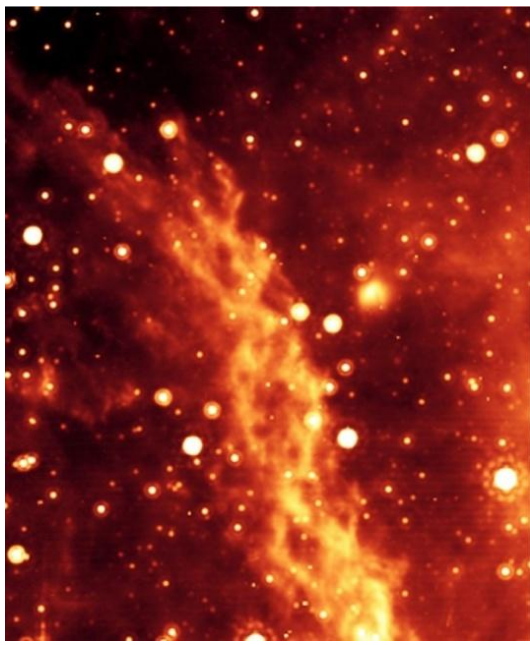
Our choice: $n=5$



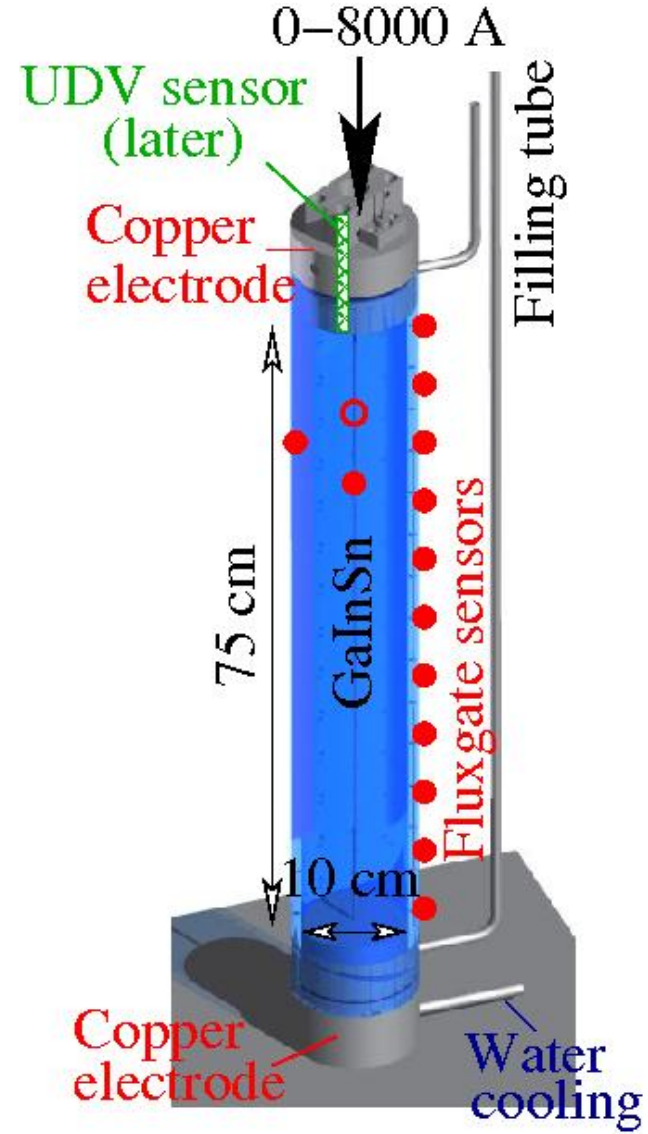
Kink-type Tayler instability (TI)

Astrophysical motivation:

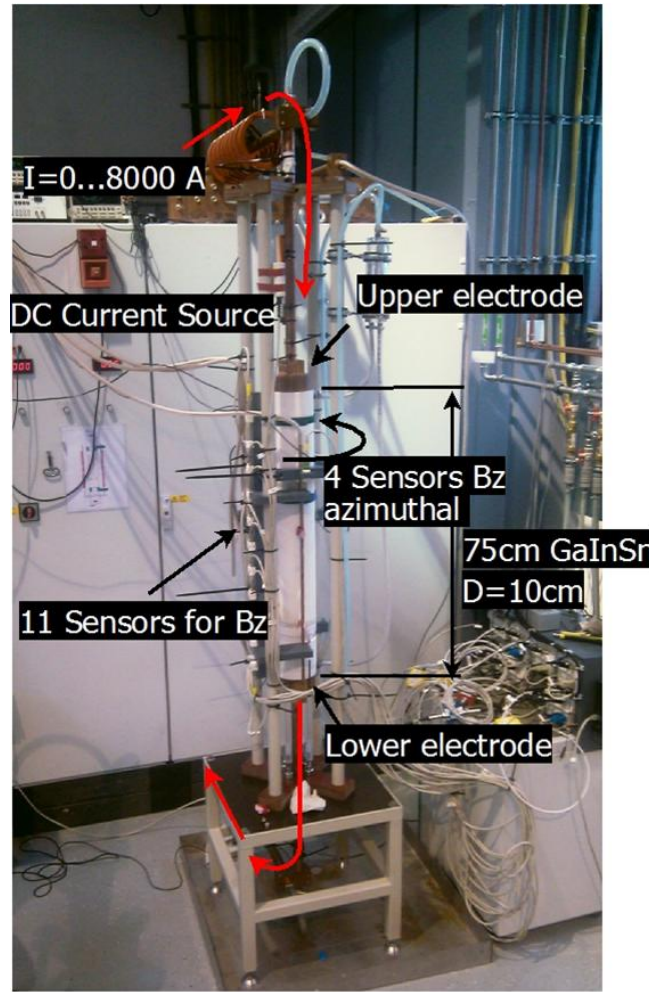
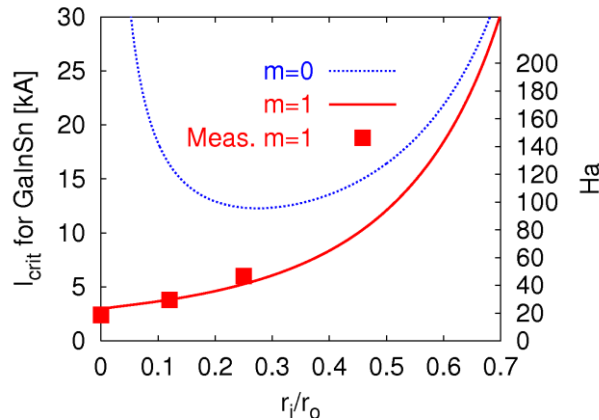
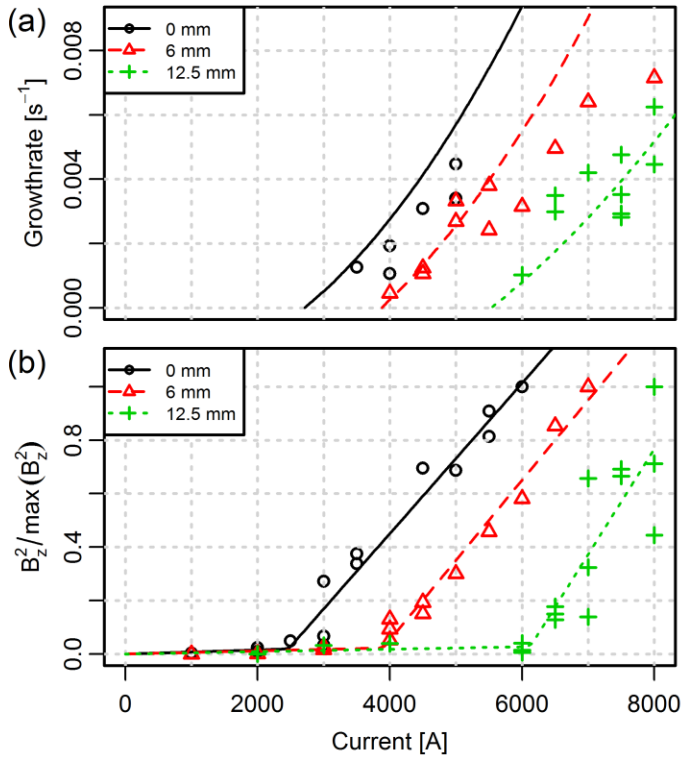
- Alternative mechanism of solar dynamo (**Tayler-Spruit dynamo**)
- Braking of neutron stars
- Structure formation in cosmic jets



Seilmayer et al.,
Phys. Rev. Lett. 108
(2012), 244501



Results of TI experiment for different r_i , and comparison with numerics

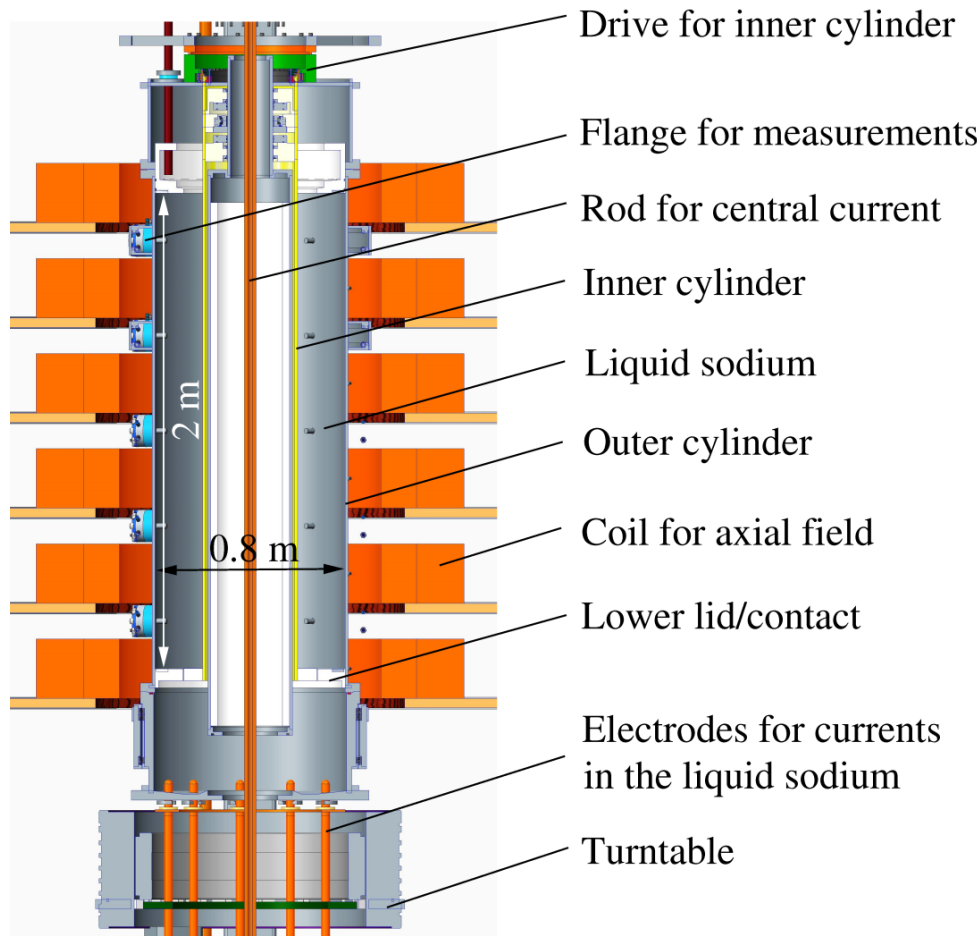


Seilmayer et al., Phys. Rev. Lett. 108 (2012), 244501

Combined MRI/TI experiment planned in the framework of DRESDYN

...will (hopefully) allow us to study helical MRI, azimuthal MRI, **standard MRI**, and their combinations with Tayler instability

- $R_{in}=0.2\text{ m}$
- $R_{out}=0.4\text{ m}$
- $H=2\text{ m}$
- $f_{in}=20\text{ Hz}$
- $f_{out}=6\text{ Hz}$
- $B_z=120\text{ mT}$
- (will need some 200 kW)
- $Rm=40$
- Lundquist=8

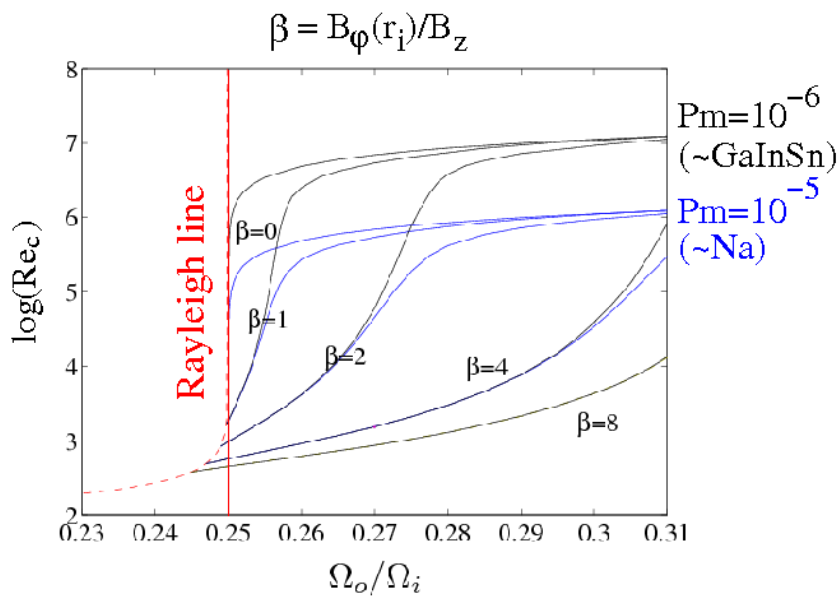


“Much as in the mid-nineteenth century, the point was missed that for fluid equations of the Navier-Stokes type the ideal limit with zero dissipation coefficients has essentially nothing to do with the case of small but finite dissipation coefficients”

D. Montgomery: Hartmann, Lundquist, and Reynolds: *The role of dimensionless numbers in non-linear magnetofluid behavior.*
Plasma Phys. Control. Fusion 35 (1993) B105-B113

Relation between standard MRI (SMRI) and helical MRI (HMRI)

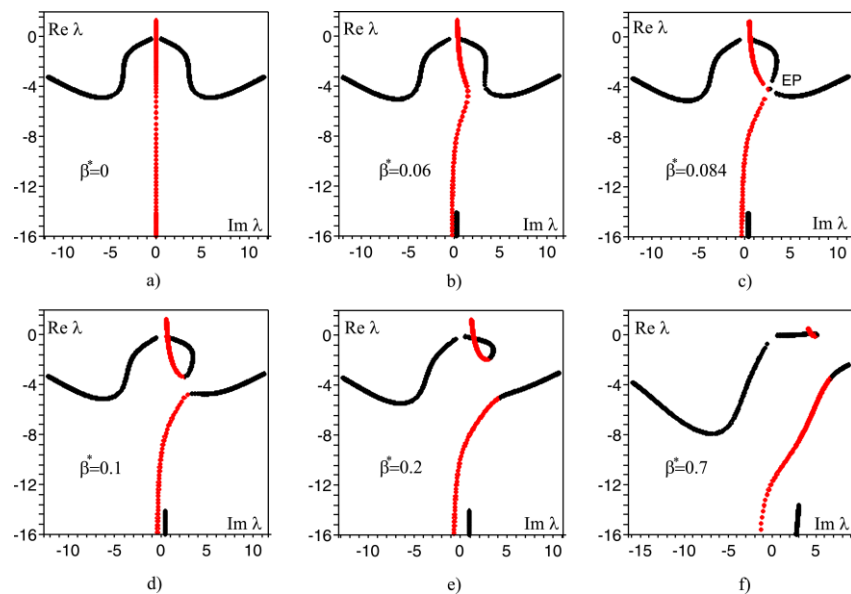
Apparent paradox: Transition between SMRI and HMRI is **continuous and monotonic**, although they represent different branches of the dispersion relation



R. Hollerbach 2008

Hollerbach and Rüdiger, PRL 95 (2005), 124501

Solution of the riddle: At small P_m the inertial mode and the slow magneto-Coriolis coalesce at an exceptional point and exchange the unstable branches



Kirillov and Stefani, *Astrophys. J.* 712 (2010), 52

MRI and TI: Viscous, resistive MHD with azimuthal wavenumber m

Navier-Stokes equation:

$$\frac{\partial \mathbf{u}}{\partial t} + \mathbf{u} \cdot \nabla \mathbf{u} = -\frac{\nabla P}{\rho} + \frac{\mathbf{B} \cdot \nabla \mathbf{B}}{\mu_0 \rho} + \nu \nabla^2 \mathbf{u}$$

Induction equation:

$$\frac{\partial \mathbf{B}}{\partial t} + \mathbf{u} \cdot \nabla \mathbf{B} = \mathbf{B} \cdot \nabla \mathbf{u} + \eta \nabla^2 \mathbf{B}$$

Viscous, resistive, and two Alfvén frequencies for axial and azimuthal field

$$\omega_\nu = \nu |\mathbf{k}|^2, \quad \omega_\eta = \eta |\mathbf{k}|^2, \quad \omega_{A_z} = \frac{k_z B_z^0}{\sqrt{\rho \mu_0}}, \quad \omega_{A_\phi} = \frac{B_\phi^0}{r \sqrt{\rho \mu_0}}$$

Dimensionless: Magnetic Prandtl, Field ratio, Reynolds, Hartmann, n

$$Pm = \frac{\omega_\nu}{\omega_\eta}, \quad \beta = \alpha \frac{\omega_{A_\phi}}{\omega_{A_z}}, \quad Re = \alpha \frac{\Omega}{\omega_\nu}, \quad Ha = \frac{\omega_{A_z}}{\sqrt{\omega_\nu \omega_\eta}}, \quad n = \frac{m}{\alpha}$$

with $\alpha = k_z |\mathbf{k}|^{-1}, |\mathbf{k}|^2 = k_r^2 + k_z^2$



Theory: Short wavelength approximation (WKB):

Hydrodynamic and magnetic Rossby numbers:

$$\text{Ro} = \frac{r}{2\Omega} \frac{\partial \Omega}{\partial r}, \quad \text{Rb} = \frac{r}{2\omega_{A_\phi}} \frac{\partial \omega_{A_\phi}}{\partial r}$$

Secular equation: $p(\lambda) = \det(\mathbf{H} - \lambda \mathbf{E}) = 0$ with

$$\mathbf{H} = \begin{pmatrix} -in \text{Re} - 1 & 2\alpha \text{Re} & \frac{i \text{Ha}(1+n\beta)}{\sqrt{\text{Pm}}} & -\frac{2\alpha\beta \text{Ha}}{\sqrt{\text{Pm}}} \\ -\frac{2 \text{Re}(1+\text{Ro})}{\alpha} & -in \text{Re} - 1 & \frac{2\beta \text{Ha}(1+\text{Rb})}{\alpha\sqrt{\text{Pm}}} & \frac{i \text{Ha}(1+n\beta)}{\sqrt{\text{Pm}}} \\ \frac{i \text{Ha}(1+n\beta)}{\sqrt{\text{Pm}}} & 0 & -in \text{Re} - \frac{1}{\text{Pm}} & 0 \\ -\frac{2\beta \text{HaRb}}{\alpha\sqrt{\text{Pm}}} & \frac{i \text{Ha}(1+n\beta)}{\sqrt{\text{Pm}}} & \frac{2 \text{Re Ro}}{\alpha} & -in \text{Re} - \frac{1}{\text{Pm}} \end{pmatrix}$$

Kirillov and Stefani, Phys. Rev. Lett. 111 (2013), 061103; JFM 760 (2014), 591

Combining MRI and TI: A chance to destabilize Keplerian profiles?

WKB-Analysis of the complete viscous and resistive MRI/TI problem for arbitrary azimuthal modes

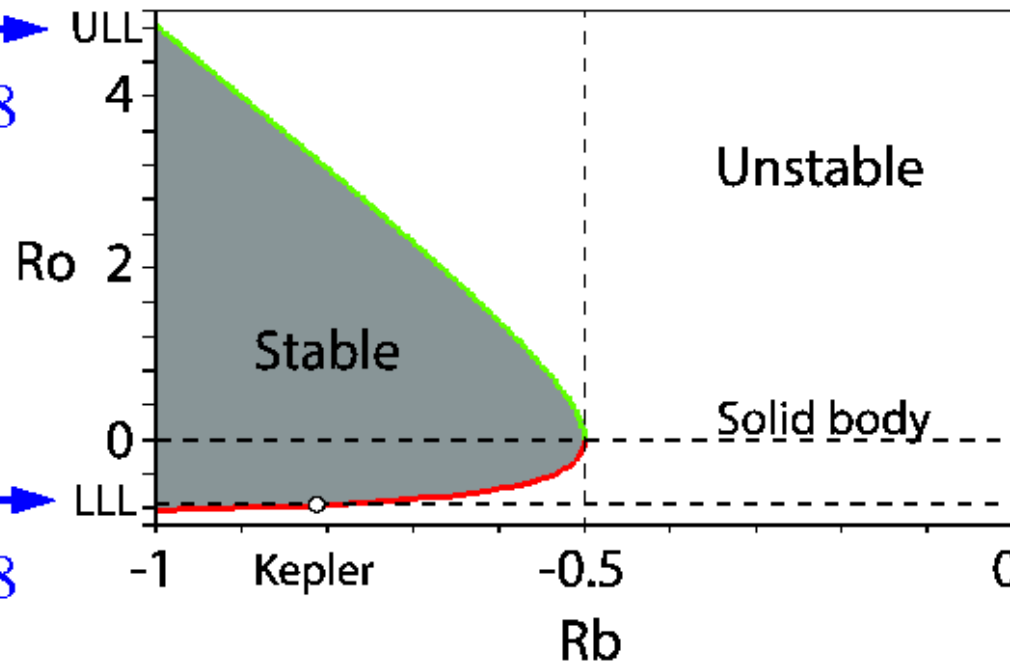
Main results:

$$Rb = -\frac{1}{8} \frac{(Ro + 2)^2}{Ro + 1}$$

Upper Liu
limit: $Ro = +4.828$

Liu, Goodman, Herron,
Ji, Phys. Rev. E 74
(2006), 056302

Lower Liu
limit: $Ro = -0.828$



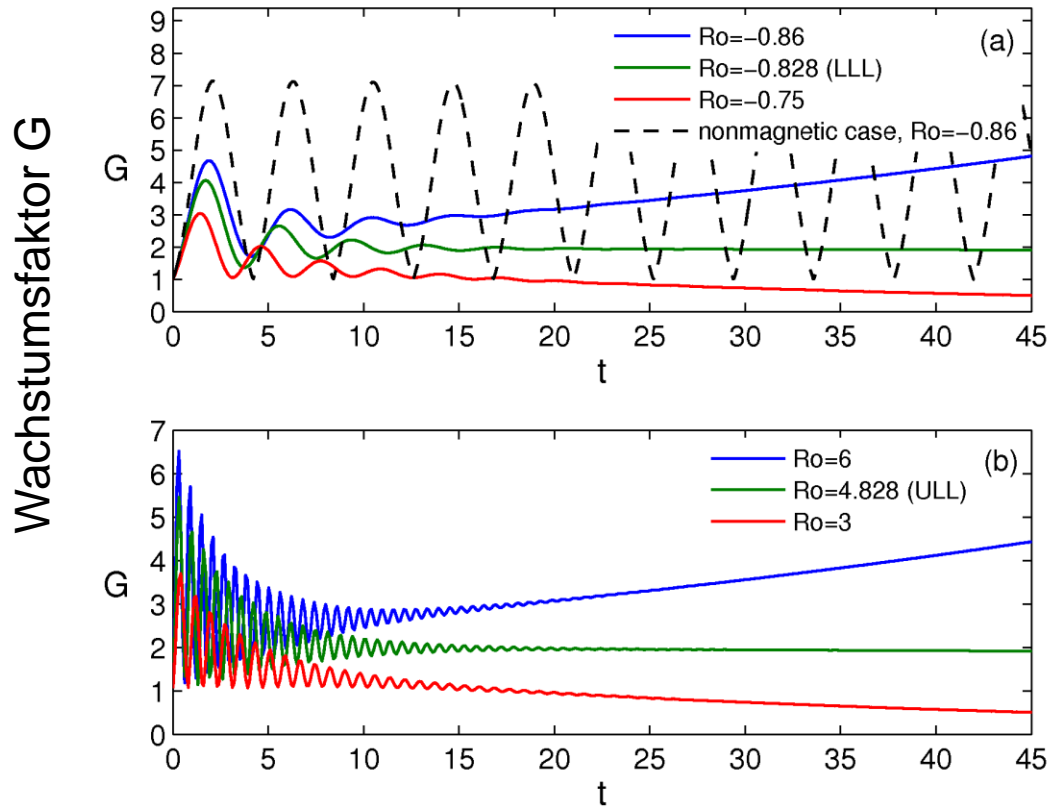
THEORY

Steepness of azimuthal magnetic field

Kirillov and Stefani, Phys. Rev. Lett. 111 (2013), 061103; Fluid Dyn.
Res. 46 (2014), 031403; JFM 760 (2014), 591

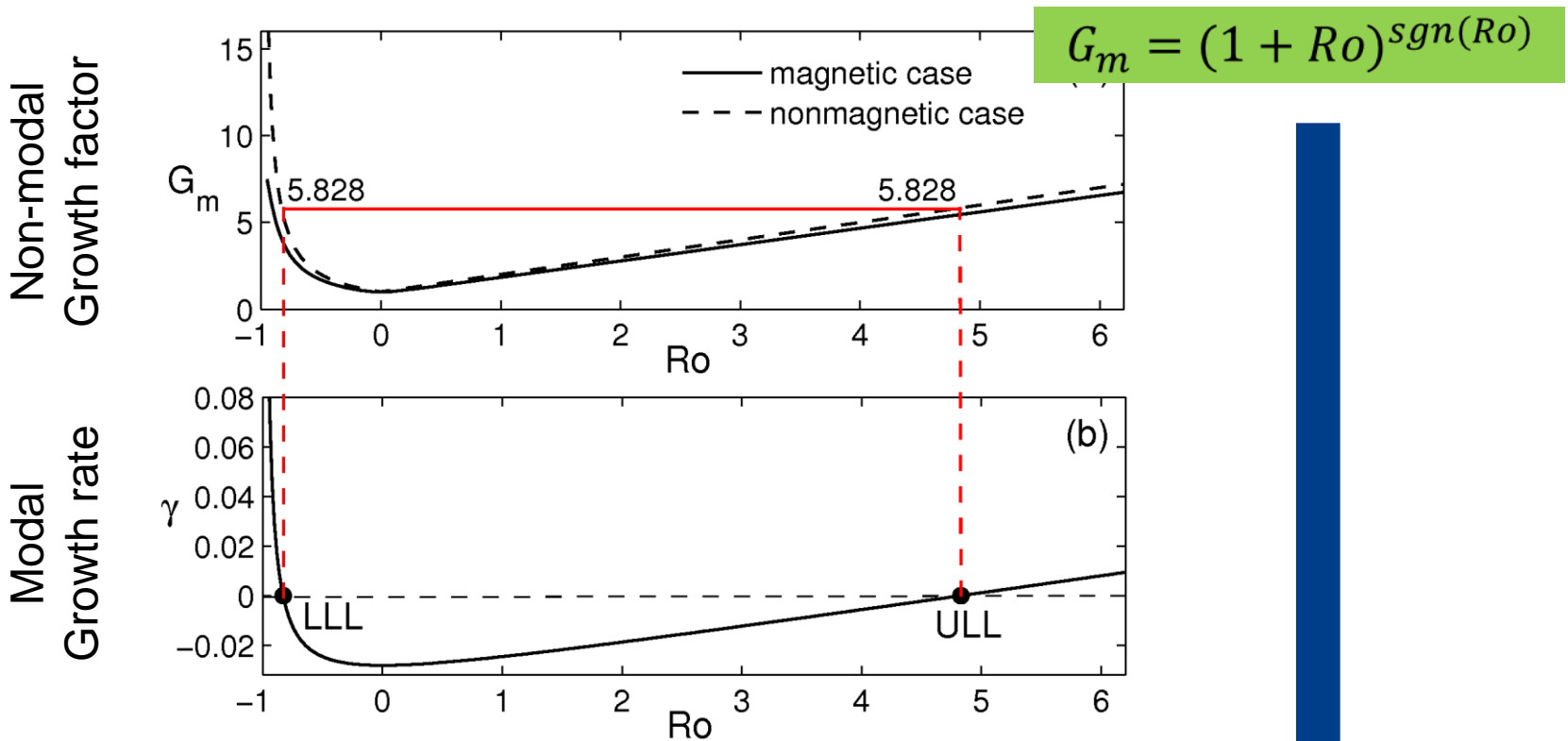
Physical background of Liu limits

Transient non-modal growth, intermediate decay, and final exponential growth of eigenfunctions of MRI



Mamatsashvili and Stefani, arXiv:1604.07205

Analytical connection between transient growth of the pure hydrodynamic case and modal growth of the HMRI



$$\gamma = \frac{Ha^2}{Re} \left[\frac{(Ro + 2)^2}{8(1 + Ro)} - 1 \right] = \frac{Ha^2}{Re} \left[\frac{(G_m + 1)^2}{8G_m} - 1 \right]$$

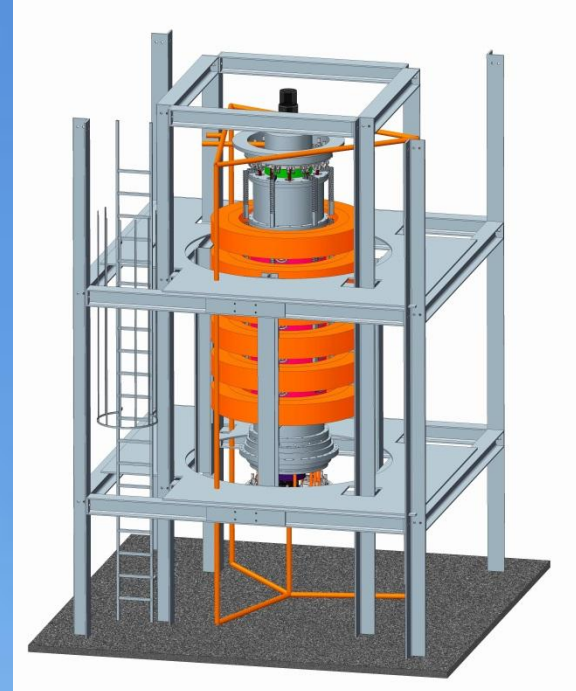
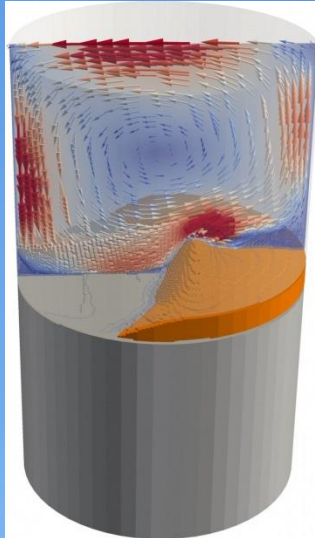
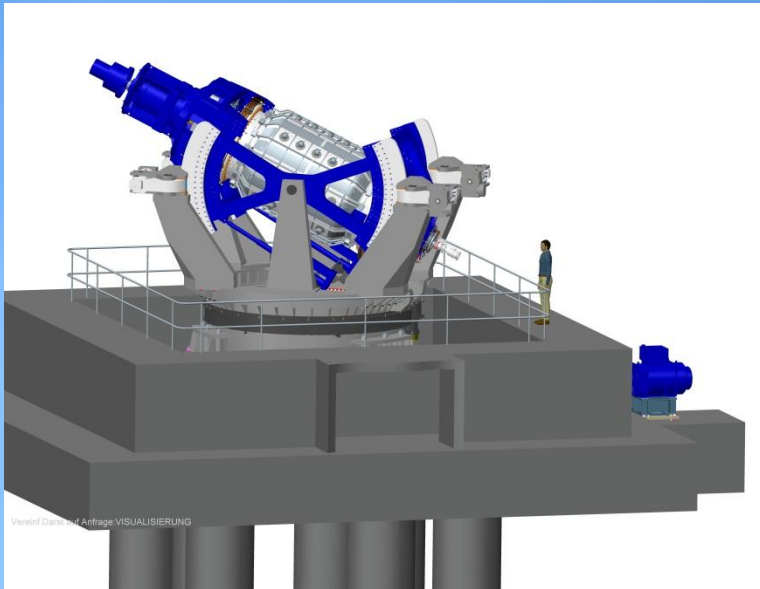


Mamatsashvili and Stefani, arXiv:1604.07205

Summary on diffusive instabilities

- HMRI and AMRI are diffusive, i.e. dissipation induced instabilities
- Chandrasekhar's equipartition solution can be destabilized by AMRI
- Presence of weak internal currents can lead to destabilization of Keplerian flows
- Flows with steep positive shear can be destabilized by HMRI and AMRI
- Very close **connection of the non-normal (transient) growth factor of purely hydrodynamic flow with the normal growth rate of (dissipation-induced) HMRI**

T
H
E
O
R
Y



Thank you for your attention